https://doi.org/10.5194/jecats-2026-15
Preprint. Discussion started: 14 August 2026

Assessing the climate mitigation potential of targeted SAF use in 2030 at Copenhagen Airport

Roland Eichinger[1], Katrin Dahlmann[1], Volker Grewe[1,2], Benedict Enderle[3], Sven Maertens[4], Shravana Kumar[4], Christian Weder[5], Wolfgang Grimme[4], Leon Müller[4], Malte Niklaß[5], and Hannes Bruder[5]

[1]Deutsches Zentrum für Luft- und Raumfahrt (DLR), Institut für Physik der Atmosphäre, Oberpfaffenhofen, Germany
[2]Faculty of Aerospace Engineering, Delft University of Technology, Delft, the Netherlands
[3]Deutsches Zentrum für Luft- und Raumfahrt (DLR), Institut für Verbrennungstechnik, Stuttgart, Germany
[4]Deutsches Zentrum für Luft- und Raumfahrt (DLR), Institut für Luftverkehr, Cologne, Germany
[5]Deutsches Zentrum für Luft- und Raumfahrt (DLR), Institut für Luftverkehr, Hamburg, Germany

Correspondence: R. Eichinger (roland.eichinger@dlr.de)

Abstract. Sustainable aviation fuels (SAFs) reduce CO_2 life-cycle emissions and the climate effect of contrail-induced cirrus cloudiness (CiC). In contrast to the CO_2 emissions of air traffic, the CiC climate effect varies strongly from flight to flight. Hence, SAF allocation to specific flights can maximise climate mitigation efforts for limited amounts of SAF, especially as long as SAF supply is meagre. In this study, we assess the climate-optimal SAF distribution for the flights departing from Copenhagen Airport (CPH) and determine the potential climate benefit achievable through this measure. The study particularly targets year 2030, when the 6% SAF mandate by ReFuelEU Aviation is expected to allow large climate benefits through targeted SAF use and time still remains for infrastructural adaptions. For this, we use the AirClim model with a refined SAF parameterisation that considers non-volatile particulate matter (nvPM) reduction dependency on SAF blending ratio. We are allocating SAF to those flights that have the largest CiC climate effect to fuel use ratio in a climatological sense. In our scenario simulations, the additional climate benefit through targeted SAF use is quantified and the tradeoff between larger SAF blending ratios for less flights as a consequence of the limited SAF amount is analysed. Targeted use of the 6% SAF can enhance the role of CiC regarding climate benefit of SAF from 20% (uniform use) to almost 50% (targeted use) when the optimal SAF blending ratio is chosen. In our results for CPH in 2030, this leads to a total additional reduction of 60 kt CO2e. However, the results show large uncertainties and strongly vary with choice of climate metric as well as with focus on long-term or short-term climate goals and depend on the specific flight plan. In addition, we quantify how much of the additional climate benefit would be sacrificed if a semi-optimal flight selection was chosen that potentially could reduce logistical cost by decreasing the number of SAF allocated flight routes. The results of this study set ground for cost-benefit analyses that take into account all airport operations associated with targeted SAF use at Copenhagen Airport.

1 Introduction

The aviation sector is transacting numerous efforts to reduce the considerable climate impact of air traffic, including both CO_2 and the much discussed non-CO_2 effects (see e.g. Lee et al., 2021). One of these efforts is the 2023 adopted ReFuelEU

https://doi.org/10.5194/jecats-2026-15
Preprint. Discussion started: 14 August 2026

Aviation regulation from the European Parliament and Council (European-Commission, 2023), which obliges all aviation fuel suppliers to provide increasing amounts of sustainable aviation fuel (SAF) to EU airports in the coming years and decades. The regulation started in 2025 with 2% of SAF, increases to 6% in 2030 and scales up rapidly thereafter until 70% in 2050. SAF is produced in multiple ways on biogenic or Power-to-Liquid (PtL) basis following requirements and criteria for sustainability certification. Currently, SAF usage is approved to a maximum blending ratio of 50% with fossil-based jet fuel depending on the feedstock-production pathway considered, with ongoing efforts to increase blending limits. As CO_2 emitted from SAF-fuelled aircraft had been absorbed by the biomass used in the SAF production, SAF strongly reduces aviation CO_2 life-cycle emissions. But additionally, SAF reduces the climate effect by contrail (condensation trail)-induced cirrus cloudiness (CiC Bock and Burkhardt, 2019; Burkhardt et al., 2018). Persistent contrails form under cold and humid enough atmospheric conditions (Schmidt, 1941; Appleman, 1953) and impact Earth's radiative properties with a net warming effect (e.g. Burkhardt and Kärcher, 2011). In particular, the decreased outgoing long-wave radiation through CiC, which is generally warming, outweighs the increased atmospheric reflectivity in the short-wave spectrum that has a cooling effect. Lee et al. (2021) quantified this net CiC effective radiative forcing to 65-70% larger than the ERF of CO_2 by past aircraft emissions, although connected with large uncertainties. As SAF on average contains less carbon (in form of aromatics, naphthalenes or other) and a higher hydrogen content (Gierens et al., 2024), SAF-fuelled aircraft emit less non-volatile particulate matter (nvPM) (Moore et al., 2017), leading to lower ice crystal number concentrations with larger ice crystals in the formed contrails (Voigt et al., 2021; Bräuer et al., 2021; Märkl et al., 2024). In consequence, this reduces the overall CiC climate effect, as these contrails are optically thinner and less persistent (Burkhardt et al., 2018; Teoh et al., 2022a; Gierens et al., 2024), and this is despite the fact that the larger hydrogen content to some degree increases persistent contrail formation (Hofer et al., 2024; Megill and Grewe, 2025).

However, in contrast to Tank-to-Wheel (TtW) CO_2 emissions of a flight, which are directly proportional to fuel use, the CiC climate effect is highly variable from flight to flight. According to a regional analysis of global chemistry-climate model simulations, Burkhardt et al. (2018) estimate that the 10% largest contrail cirrus clusters are responsible for 42% of the short-wave radiative impact and that only few contrail-cirrus outbreaks are responsible for most of the CiC radiation effect. Teoh et al. (2024) state that globally around 1.5-3% of flights are responsible for 80% of the climate effect by CiC, although these results are likely to be somewhat overestimated due to a lack of saturation effects. The climate impact of CiC mainly depends on the atmospheric conditions, but contrail formation itself also strongly depends on emission strength and composition at the particular point in time. For this, aircraft and engine properties, thrust setting and fuel characteristics play crucial roles. In a situation with limited amounts of SAF, it may therefore be climatically beneficial to allocate larger ratios of SAF to fewer specific flights instead of distributing it uniformly to all flights. If large SAF ratios were allocated to the climatically most impactful flights regarding the CiC effect, climate mitigation efforts could be maximised for limited amounts of SAF. For this, the maximum additional climate benefit through targeted SAF use could be achieved by choosing those flights with the largest CiC climate impact in relation to the flights' fuel use. As the actual meteorological conditions during flight execution (particularly those in future years) are inherently unpredictable, we conduct the analysis in a climatological manner rather than in a deterministic weather forecasting context. Accordingly, the focus is to identify flights that are statistically most prone to exhibiting the largest CiC climate effect to fuel use ratio. The question therefore is, how much more climate benefit can be

https://doi.org/10.5194/jecats-2026-15
Preprint. Discussion started: 14 August 2026

gained at an airport through targeted SAF use instead of distributing it uniformly to all flights? Moreover, what is the optimal SAF blending ratio for this undertaking, referring to the tradeoff that the larger the chosen blending ratio, the fewer flights can receive SAF? Several related studies on the topic have already been carried out. For example, Teoh et al. (2022b) have analysed the climate mitigation potential of targetet SAF deployment to North Atlantic flights and Quante et al. (2025) investigated 84 winter time demonstration flights between Stockholm and Copenhagen. Woeldgen et al. (2025) quantified contrail mitigation potential and fuel supply chain costs in a general manner for various targeted SAF use strategies at EU and UK airports. In the present study, we complement these studies by specifically targeting the flights departing from Copenhagen Airport (CPH) in the year 2030 and assess the optimal blending ratio, to lay ground for a dedicated cost-benefit analysis and possible action resting upon the results.

Within the ALIGHT project, CPH worked towards the introduction of sustainable aviation solutions for the future. One of the project foci is the infrastructure for SAF at the airport. To achieve the optimal solutions for this, a prerequisite is knowledge of the climate-optimal SAF distribution at the airport. This includes choice of flights for SAF allocation and also the SAF blending ratio that promises the largest climate benefit. Our analysis specifically focuses on year 2030, when targeted SAF use promises large climate benefits due to the 6% SAF quota and infrastructural measures at CPH could still be conducted for operational realisation. The results of this study are crucial for a cost-benefit analysis additionally taking into account relevant aspects of airport infrastructure and operations to assess practical feasibility (Müller et al., 2026). In the present study, we lay the ground for this analysis with a climate effect analysis of all flights departing from CPH varying the SAF blending ratio in dedicated flights. The paper starts with the description of the concept and the explanation of the scenario selection in Sect. 2. Subsequently, the used emission inventory, the climate effect model, the simulation setup, the used climate metrics and the refinement of the SAF parameterisation are described in Sect. 3. Sect. 4 comprises the results starting with the effect of certain SAF blends tanked to all flights and then proceeds to allocation of certain SAF blends to the most effective flights and the additional climate benefit. Here, we also show sensitivities and coherences between CiC-intense flights and other flight specifics such as aircraft size, mean flight latitude and cruise altitude. The last part of Sect. 4 studies what climate effect targeted SAF use could achieve without taking the ratio with fuel use, for the sake of easier logistics at the airport. We discuss the paper results in Sect. 5 before we end with a presentation of the main conclusions.

2 Concept and scenario selection

There are a number of concepts how to distribute SAF available at an airport to the departing flights. These concepts generally are associated with a tradeoff between the climate benefit they provide and the logistical effort they require (see Fig. 1). The extreme case with the lowest climate benefit and lowest effort is even distribution of SAF to all flights. On the other extreme, a concept can be thought of that includes actual weather forecast to SAF fuelling, meaning that a flight receives SAF if it is predicted to fly through an ice-supersaturated region, hence is prone to producing warming CiC. However, this concept is logistically extremely complex and the uncertainties in today's weather forecasts (von Bonhorst et al., 2025) and CiC climate effects are subject to large uncertainties (Lee et al., 2021). Hence, it is currently unclear to what extend and with what risk those

https://doi.org/10.5194/jecats-2026-15
Preprint. Discussion started: 14 August 2026

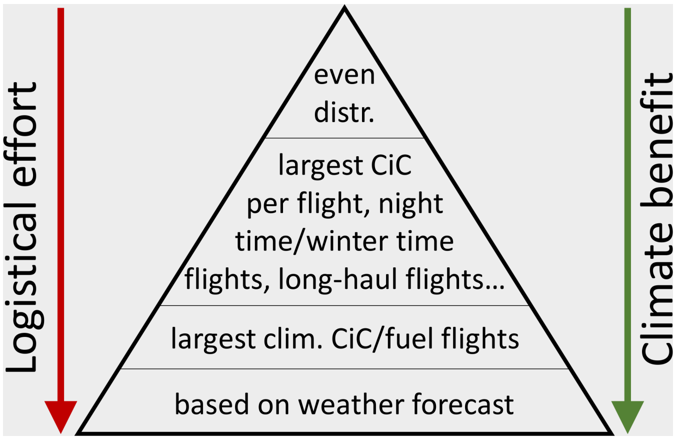

Figure 1. Tradeoff for distribution of limited amounts of SAF to individual flights.

procedures can be planned (Quante et al., 2025; Borella et al., 2026; Staniaszek et al., 2026). Intermediate solutions comprise applying SAF predominantly to night-time or winter season flights (Quante et al., 2025; Woeldgen et al., 2025), to long-haul flights or to those flights with the largest climatological CiC effect (Quante et al., 2024). It is likely that the climatological effectiveness of the particular one of these measures differs for the specific airport flight plan. However, a measure that is most certainly advantageous over these is to allocate higher SAF blends to those flights with the largest CiC climate impact in relation to the fuel use of the flights.

Despite its large flight-to-flight variability, the CiC climate effect can be approached climatologically, accounting for the probability of ice-supersaturated conditions at a given location (latitude, longitude, altitude) and the climatological response of a formed contrail. This way, the climate impact including non-CO_2 effects of a specific flight route can be estimated assuming that it takes place on every day and all occurring weather situations and hence without knowledge of the actual weather situation. A suitable climate response model and consideration of individual flight route emissions is needed for that. In addition, a SAF parameterisation to estimate the influence of SAF on the CiC effect needs to be applied to assess the question. We therefore here use the AirClim model (Grewe and Stenke, 2008; Dahlmann et al., 2016) with a refined SAF parameterisation to study the additional climate gain through the reduced CiC climate effect by targeted SAF use for all flights departing from one airport. The model, the SAF parameterisation and the emission inventory are described in Sect. 3.

To follow this concept, in the present study we first simulate the reference case with conventional jet fuel only (No SAF or 0% SAF) and the uniform case in which all flights receive the same SAF blending ratio of 6%. Then, we use the 0% SAF case to find the most CiC-intense flights in relation to fuel consumption. This means, we assort the flights by their CiC effect to fuel use ratio to assign the available SAF at the airport to the first flights in this list. Hence, only the first flights in the list receive SAF blends higher than the 6% until the total available SAF at the airport is used up. The basics of this concept are outlined in Fig. 2. To detect the blending ratio that yields the maximum climate benefit, we perform the SAF distribution in 6 different

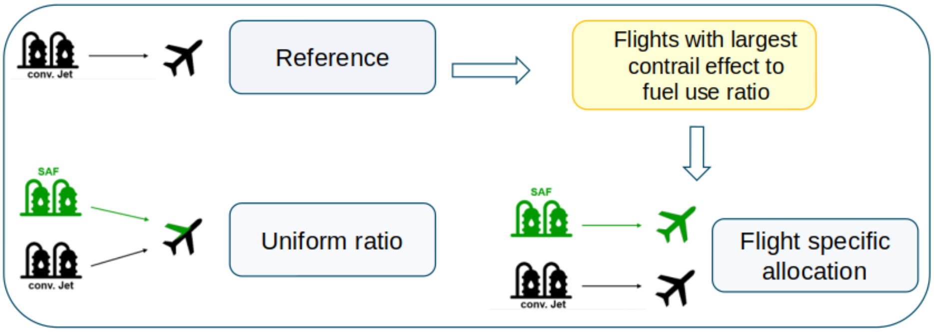

Figure 2. Schematic of the concept for the climate impact analysis of targeted SAF.

scenarios with 30%, 40%, 50%, 60%, 70% SAF blends and 100% SAF, respectively. Logically, the larger the blending ratio, the fewer flights receive SAF.

We chose to analyse year 2030 as we expect a larger additional climate benefit through targeted SAF use when only little fractions of SAF are available (and demanded by the RefuelEU aviation regulation European-Commission, 2023). In 2030, a fraction of 6% SAF at the airport is required by the regulation. Moreover, the time span from today to 2030 would still allow implementation of such a system at CPH airport in case it turns out to be overall beneficial, including the results of an economic cost-benefit analysis (Müller et al., 2026). This concept also means that the total SAF available at CPH for our simulations is assumed to be 6% of the total fuel use by all flights departing from the airport in year 2030.

The AirClim climate effect simulations are carried out with so-called pulse emissions. This means the emissions happen only in year 2030 but their climate impact is calculated for the subsequent decades depending on the time horizon in the climate metric chosen (see Sect. 3.2). For these calculations, the flights at CPH in 2030 are estimated based on the year 2019 and a so-called middle of the road climate scenario for background climate conditions (see the next sections 3.1 and 3.2, respectively, for more details on the experimental set-up).

3 Data and model

3.1 Emissions inventory

For this study, we represent the 2030 air traffic by the base year air traffic of 2019, the year before the COVID-19. Air traffic strongly reduced in 2020 due to the pandemic and recovered afterwards such that the 2019 air traffic can be seen as a reasonable reference for the year 2030. As the focus of this study is analysing effects of targeted SAF use we refrained from including other elements that could distort clear identification of the non-CO_2 effects, such as traffic growth or replacements in the aircraft fleet over time, which would involve additional uncertainty. The annual route network of CPH airport, that consist of a flight schedule with 129631 instrument flight rules (IFR) flights all departing from CPH, is taken from Sabre Market Intelligence

https://doi.org/10.5194/jecats-2026-15
Preprint. Discussion started: 14 August 2026

database (Sabre MI, 2019) and contains information on origin and destination airport, aircraft type, departure day and time, operating airline, assigned cruise flight level and seat load factor.

We created an emission inventory containing 3-dimensional distributions of CO_2, NO_x (as NO_2 mass-equivalent), H_2O emissions and the flown distance per grid cell (see exemplarily in Fig. 3). The applied methodology is described in greater detail in the following. First of all, the annual route network of CPH airport is aggregated and missions with the same destination airport, aircraft type, seat load factor and cruise flight level are summarised to 5160 flight missions (in the following also called flight routes). Standardised four-dimensional aircraft trajectories, that contain information on e.g. speed and altitude profile, climb and descent rate, engine thrust, fuel and emission flows along the most relevant flight phases have been preprocessed with the DLR Trajectory Calculation Module (TCM) based on Base of Aircraft Data Model family 4 (BADA4) aircraft performance models (Nuic et al., 2010), and the total-energy-model (Linke, 2016). The required atmospheric background data come from ICAO International Standard Atmosphere (ISA) (ICAO, 1993). The trajectories have been stored in a database of Reduced Emission Profiles (RedEmP) for all available aircraft types, various discrete flight distances in steps of 100 NM, several seat load factors and cruise altitudes. Those RedEmPs are applied in this study for aircraft trajectories in order to reduce the computational effort. To complete the coverage of the fleet at CPH, previous modeled simplified trajectory data based on BADA3 aircraft performance models are used supplementary (Nuic et al., 2010).

We assume stoichiometric combustion and apply constant emission indices of 3.159 kg CO_2/kg fuel and 1.237 kg H_2O/kg fuel for Jet A-1 fuel from Wilkerson et al. (2010). NO_x emissions depend on both the engine combustor temperature and flight phase and are non-linear with fuel burn. Engine-specific NO_x emission indices from test bench measurements are provided in the ICAO Engine Emission Databank (ICAO, 2012; EASA, 2023) for state-of-the-art jet engines for various thrust settings as defined in ICAO Landing-Takeoff-Cycle (LTO) (ICAO, 2008). For extrapolation to in-flight conditions, the DLR fuel flow correlation method is applied (Deidewig et al., 1996), using ISA conditions modified by an altitude-dependent humidity profile (ICAO, 1993; Schaefer and Bartosch, 2013). For the remaining aircraft, where no specific NO_x EI data are available, a constant EI_{NO_x} of 14.1 g NO_2/kg fuel, derived as a fleet-average from Wilkerson et al. (2010) is used.

To ensure a more realistic routing, a sample of real flight path profiles from ADS-B data from the OpenSky Network (Schäfer et al., 2014; Strohmeier et al., 2021) and model3 data from the Demand Data Repository 2 from EUROCONTROL (Urjais, 2022) for year 2019 are used for georeferencing the flight trajectories. For missions where no flight path data are available, the great circle route is used instead.

In order to consider head and tail wind effects on the aircraft's ground distance, the method of Swaid et al. (2024) is applied to scale the ground distance for each flight path with the average of the annual statistical wind impact on ground distance. We apply this method, using the aircraft's true air speed from the RedEmP, the actual heading from the mission-specific flight path data and local annual wind statistics along the flight path segments that consist of wind speed and direction data with a horizontal resolution of 0.25° × 0.25° on various pressure levels for 0-, 6-, 12- and 18-UTC of every day within the year 2019 from ERA-5 reanalysis data (Hersbach et al., 2023).

For each mission within the annual CPH network, the **G**lobal Ai**r** Traffic Em**i**ssion **D**istribution **Lab**oratory (GRIDLAB) from DLR is used to pick the best-fitting RedEmP with regard to the mission-specific seat load factor, cruise flight level and the air

https://doi.org/10.5194/jecats-2026-15
Preprint. Discussion started: 14 August 2026

distance of an appropriate randomly selected flight path from the database. Subsequently, the cruise phase of the RedEmP with constant speed and fuel flow is truncated to the actual wind-corrected air distance and the restricted climb and descent phases are adjusted to fit to the local airport elevation, as given in the applied airport database (openflights.org, 2026). Afterwards, the adjusted RedEmP is georeferenced along either the selected flight path or otherwise great circle route on the assigned constant cruise altitude and projected on a 3-dimensional numerical grid with a resolution of 0.25° × 0.25° × 1000ft. The methodology of the DLR emission model GRIDLAB and RedEmP is described in detail in Righi et al. (2026). To consider air traffic management (ATM) effects and inefficiencies implicitly, the RedEmPs are projected on up to five different flight paths per mission and their emission amounts are weighted evenly and summed up. Finally, the 3-dimensional emission grid of each mission is scaled-up with its annual frequency. In the next step, these data are read in by the AirClim model and further used for climate effect calculations (see Sect. 3.2).

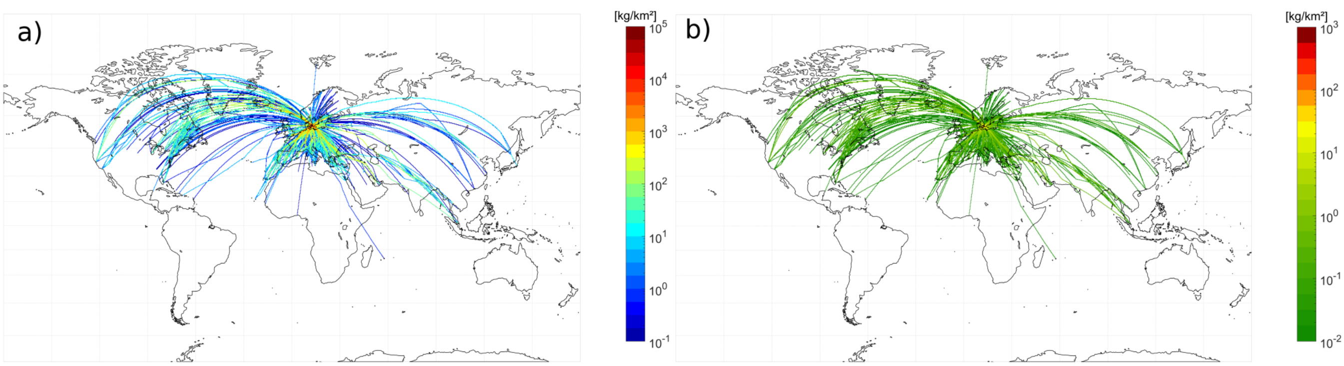

Figure 3. Longitude-latitude map of vertically aggregated annual total aviation emissions for all flights departing from CPH in 2019 for a) CO_2 and b) NO_x.

3.2 Model, setup and metrics

AirClim is a climate response model that can be applied to provide an estimate of the climate effects of aircraft CO_2 and non-CO_2 emissions at a specific location in a computationally fast though non-linear way. The model has been develeoped by Grewe and Stenke (2008), continuously refined further since then and used for multiple studies (e.g. Dahlmann et al., 2016; Linke et al., 2017; Matthes et al., 2021; Grewe et al., 2021; Zengerling et al., 2022; Dahlmann et al., 2023). AirClim includes pre-calculated atmospheric impact data to calculate for example the aviation climate impact for a multitude of emission inventories and it can be used to evaluate the climate effect of basic aircraft and engine configurations and general operational strategies. For the precalculated data, idealised emission regions with normalised emission strength were defined on 84 grid boxes (7 latitudes & 12 altitudes). For each of the idealised emission regions, a chemistry-climate simulation using E39/CA (Stenke et al., 2008) was employed with normalised emissions to obtain the chemical perturbations and radiative forcing of ozone (O_3), methane (CH_4) lifetime and water vapour (H_2O). For CiC, simulations with ECHAM4-CCMod (Burkhardt and Kärcher, 2009) were used to combine 3-dimensional probability distributions for the formation of contrails with the flown distances to estimate

https://doi.org/10.5194/jecats-2026-15
Preprint. Discussion started: 14 August 2026

the local climatological contrail coverage and RF to best represent the ECHAM4-CCMod data. The model is verified against independent modelling data using the inventories that includes flight altitude changes (Dahlmann et al., 2016).

The results of these detailed simulations constitute the precalculated atmospheric input data for AirClim. AirClim combines these computing time expensive precalculated data with air traffic emission data in order to calculate composition changes, radiative forcing and near surface temperature changes caused by these emissions. This way, AirClim is used to calculate the temporal development of aviation induced radiative forcing (RF) as well as the resulting near surface temperature change for a given temporal evolution and spatial distribution of aviation emissions for CO_2, H_2O, NO_x (O_3, Primary Mode Ozone (PMO), CH_4) and CiC. With AirClim, the aviation climate impact is estimated on a climatological basis, meaning that it captures the average of the impacts of all weather situations that occur during a year. AirClim can account for different propulsion types as it includes the probability of fulfilling the Schmidt-Appleman criterion (SAC) in dependency of the overall propulsion efficiency, lower heating value of the fuel (LHV) and emission index of water vapour.

In our study, we apply a so-called 'wing span parameterisation' that has been integrated and used by Bruder et al. (2026). The parameterisation describes the dependency of the CiC climate effect on the aircraft size using the wing span b as proxy as derived from a limited set of high-resolution contrail-cirrus simulations by Unterstrasser and Görsch (2014). For a given soot emission index, a higher fuel consumption implies a larger number of ice crystals in the contrail. Moreover, larger and heavier aircraft induce stronger wake vortices, which descend further down and increase the contrail dimensions after the vortex phase. Both aspects have been shown to have a long-lasting impact on the properties of the evolving contrail-cirrus. In Unterstrasser and Görsch (2014), the aim was to demonstrate the long-lasting impact of the aircraft type on contrail-cirrus properties, but no systematic survey was performed and the data set is limited. Hence, the correction formula should be seen only as a rough first-order estimate of the influence of the size of conventional aircraft on contrail radiative properties. The parameterisation follows

$$f_{ACsize}(b) = \frac{v + w \cdot b}{v + w \cdot b_{ref}}, \qquad \text{where } b \in [20\,m, 80\,m], b_{ref} = 38\,m, v = 0.43 \text{ and } w = 0.0287\,m^{-1}. \tag{1}$$

More details on this wing span parameterisation can be found in the supplement of Bruder et al. (2026). For the present study, the wing span parameterisation proved useful in particular for assorting the flights according to their CiC effect to fuel use ratio. Without the wing span parameterisation, the CiC effect of some flights with small aircraft was overestimated, which could to some degree be improved by this measure (not shown).

For the purpose of this study, we apply the 2019 base year air traffic emission inventory described in Sect. 3.1 as pulse emissions in the year 2030. We use the SSP2-4.5 (Shared Socioeconomic Pathway with an additional radiative forcing of 4.5 W/m^2 by the year 2100) climate scenario (Riahi et al., 2017) to determine the background climate conditions, in particular the CO_2, N_2O (accounting for cross-dependencies in the CH_4 RF) and CH_4 mixing ratios in AirClim from 2030 to 2130. SSP2-4.5 describes a medium pathway of future greenhouse gas emissions, which assumes that climate protection measures are being taken. The ReFuelEU SAF mandate of 6% in 2030 implies for our study that the total available SAF at the airport is

https://doi.org/10.5194/jecats-2026-15
Preprint. Discussion started: 14 August 2026

6% of the total fuel use of all flights departing from CPH. As explained in Sect. 2, the climate effect of the pulse emissions of the aggregate of all flights departing from CPH in 2030 with varying fuel specifics will be assessed.

Based on the AirClim results, any climate metric, such as RF (radiative forcing), GWP (global warming potential), GTP (global temperature potential) and ATR (average temperature response) can be directly calculated for all time horizons. In the present study, we use EAGWP (Megill et al., 2024), which is the efficacy-weighted (E) absolute (A) GWP. This integrated climate metric has been chosen by the EU Commission as the standard for the monitoring, reporting and verification (MRV) system that is currently being implemented (European-Commission, 2024) to track EU-wide aviation non-CO_2 emissions for possible future inclusion in the EU-ETS. Moreover, the analysis by Megill et al. (2024) showed that this metric fulfills the criteria necessary to represent aviation climate effects well. We here use the efficacy values as recommended by Eichinger et al. (2025) to the European Union for establishment of the non-CO_2 aviation MRV system that base e.g. on studies by Ponater et al. (2006); Richardson et al. (2019); Bickel et al. (2020, 2025) and Rap et al. (2010), namely 1.00 for H_2O, 1.05 for O_3 as well as for PMO, 1.04 for CH_4 and 0.37 for CiC. In integrated climate metrics, longer time horizons represent better the impacts of both short-lived climate forcers, such as CiC and ozone and long-lived climate forcers such as CO_2.

The time horizon is a trade-off between incorporating the long-term response to an emission and ensuring the predictability and accuracy of a future emission scenario. Megill et al. (2024) explain that integrated climate metrics generally require longer time horizons to account for the atmospheric radiative forcing and temperature adjustment. Hence, the primary time horizon in this study is 100 years. To assess the robustness of the results, we additionally use the climate metrics ATR and AGWP. The latter allows direct analysis of the influence of using efficacies. Moreover, we apply EAGWP also with the 2 time horizons 20 and 50 years. The output of the climate metric computations are then translated to CO_2-equivalents (CO2e) to obtain a common ground for comparisons and to allow direct monetisation of the results. A CO2e is the climate impact of a climate species relative to the climate impact of one kg CO_2. The CO2e represents the amount of CO_2 which causes the same climate impact for the given climate metric.

3.3 Parameterisation of fuel-dependent emissions of particulates

Non-volatile particulate matter (nvPM) emitted by aircraft engines enhance ice crystal nucleation, thereby fostering contrail formation. Burkhardt et al. (2018) showed that the impact of soot emission reductions and the resulting decrease in initial ice crystal numbers have a non-linear effect on RF. In AirClim, a nvPM reduction therefore leads to a reduction of CiC RF following the relation

$$f(RF_{CiC}) = 0.92 \cdot arctan(1.9 \cdot EI_n^{0.74}), \qquad (2)$$

where EI_n denotes the nvPM emission indices. This relation was developed by Grewe et al. (2021) and it bases on data from the study by Burkhardt et al. (2018). The approach assumes a linear relation between ice crystal and nvPM number concentrations, which is appropriate in the soot-rich regime. The approximation implemented in the AirClim model has been applied by

https://doi.org/10.5194/jecats-2026-15
Preprint. Discussion started: 14 August 2026

Grewe et al. (2021) studying mitigation scenarios of the climate impact of aviation emissions.

So far, in AirClim the nvPM reduction through SAF was implemented directly related to the SAF blending ratio, i.e. a SAF blending ratio of $X\%$ lead to a nvPM reduction of $X\%$. For the present study, however, we have further developed the approach by a suitable correlation to estimate changes in nvPM emissions as a function of SAF blending ratios. The correlation by Teoh et al. (2022b), which partly bases on Brem et al. (2015) estimates the relative reduction in nvPM emission indices (EI_n in %) based on two primary factors: the difference in hydrogen content ΔH between conventional jet fuel (as reference value for ΔH of conventional jet fuel, 13.80% is used Teoh et al., 2022b) and the SAF blend and the current engine thrust setting $\hat{F}$ (in % of the maximum value). The correlation, calibrated against experimental data, is extrapolated for H-content differences and it is given by:

$$nvPM\ EI_n[/\ \%] = \begin{cases} \left(\alpha_0 + \alpha_1 \hat{F}\right) \cdot \Delta H, & \text{when } \Delta H \leq 0.5\% \\ \left(\alpha_0 + \alpha_1 \hat{F}\right) \cdot \Delta H \cdot e^{(0.5-\Delta H)\cdot 0.5}, & \text{when } \Delta H > 0.5\% \end{cases} \tag{3}$$

where $\alpha_0 = -114.21$ and $\alpha_1 = 1.06$. The resulting reductions in EI_n across thrust settings from 10% to 100% are illustrated in Fig. S3 of Teoh et al. (2022b).

As we here focus on SAF deployment scenarios for 2030, we intent to estimate the mean properties of SAF blends available specifically in that year to develop the emission reduction correlation. According to the ReFuelEU Aviation blending mandate, 25% of the SAF supplied in 2030 must consist of renewable fuels of non-biogenic origin, such as Power-to-Liquid (PtL) products. Given current technological maturity, it is assumed that the remaining 75% will primarily consist of bio-based SAF produced via the HEFA (Hydrotreated Esters and Fatty Acids) pathway. Among PtL technologies, the Fischer-Tropsch (FT) process is considered the most mature and therefore most likely to dominate PtL supply in this time frame. Based on these assumptions, we extracted data for the H-content of currently available HEFA and FT fuels from the SimFuel[1] database, resulting in a total of 17 data points for H-content. These values were then weighted according to the ReFuelEU blending quota and further adjusted by the respective fuel densities to yield a virtual mean neat SAF for 2030. The resulting average H-content is $H_{SAF,2030} = 15.33\,kg/kg$ and the average density is $\rho_{SAF,2030} = 755\,kg/m^3$

Using the corresponding average values for conventional Jet A-1 fuel as reported by Teoh et al. (2022a) ($H_{Jet\ A-1} = 13.8\,kg/kg$, $\rho_{Jet\ A-1} = 798\,kg/m^3$), we calculated SAF blend properties for 2030 for a range of blending ratios and inserted them into the original correlation by Teoh et al. (2022a). Reformulation as a function of SAF blend ratio then yields a derived expression for nvPM EI_n reduction specific to expected SAF blends in 2030. Fig. 4 shows the resulting correlation at a representative engine thrust setting of $\hat{F} = 30\%$. Within the context of the available data, this correlation is considered valid for blend ratios up to 73%. In the AirClim model, the relation is represented through a scaling factor on the nvPM depending on the SAF ratio. In our analyses, we consider SAF blending ratios of 6%, 30%, 40%, 50%, 60% and 70% as well as 100% SAF, which according to the data in Fig. 4 yields nvPM emission index reductions of 7.2%, 36.5%, 46.7%, 54.4%, 60.8%,

[1] SimFuel is a software platform currently under active development serving as a comprehensive tool for the assessment of SAFs across various use cases (see Enderle et al., 2022; Bauder et al., 2022)

https://doi.org/10.5194/jecats-2026-15
Preprint. Discussion started: 14 August 2026

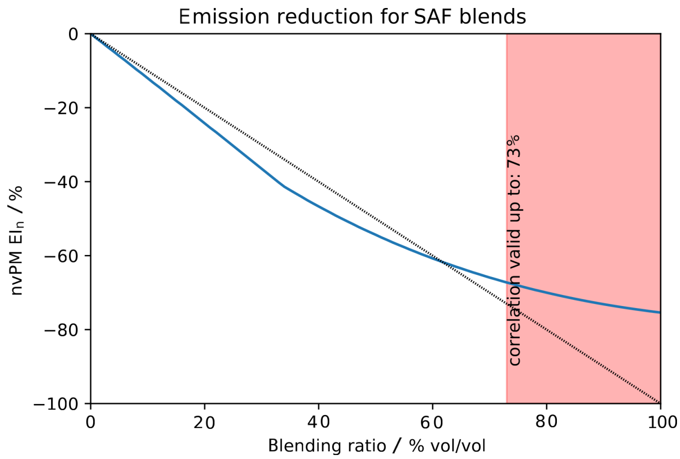

Figure 4. Reduction of nvPM emission index in dependence of SAF blending ratio based on Teoh et al. (2022a). SAF blend assumptions for 2030 are 75% bio and 25% PtL and a representative engine thrust of 30% is assumed. The relation is valid up to 73% SAF blend. Previously, the dottet 1-to-1 line was used in AirClim.

65.9% and 75.4%, respectively. In our study, the 100% SAF case is used for purpose of sensitivity analysis, showing what would happen if the relation was extended outside of the validity range.

In AirClim, the SAF blending ratio can be varied on flight, fleet or global basis. For the simulations in this study, we run the model with 8 different fuel specifications, namely with the standard settings representing no SAF use and the 7 different SAF blending ratios mentioned above. This means that in these simulations, all flights departing from CPH are fuelled with the corresponding SAF blending ratios, the merging of the targeted SAF flights with regular flights in the later results section is performed in a data postprocessing step only.

To accurately quantify the embodied life-cycle CO_2 emissions of SAF, life-cycle assessments have been performed on a wide range of SAF in recent years. The CO_2 life-cycle reductions vary largely between the different SAF types such as the HEFA pathway, waste feedstocks such as used cooking oil, agricultural residue, forestry residue and tallow as well as SAF derived from primary product feedstocks including canola, camelina, jatropha, and pennycress and other approved SAF production pathways such as Fischer-Tropsch and Alcohol-to-Jet (see e.g. Bell et al., 2025). IATA (2018) state that the use of sustainable aviation fuel has been shown to provide significant reductions in overall CO_2 life-cycle emissions compared to fossil fuels, up to 80%.

In our AirClim simulations, SAF is therefore assumed to be 80% CO_2-neutral, which reduces the CO_2 emissions with the blending ratio, down to 20% for 100% SAF flights. This assumption might not be generally representative, however, a more nuanced consideration of the effect is not relevant for the present study. Firstly, predicting the CO_2 life-cycle reductions of SAF in 2030 bears large uncertainties that are out of scope for this work. And secondly, as we here focus on the additional

https://doi.org/10.5194/jecats-2026-15
Preprint. Discussion started: 14 August 2026

climate benefit through the reduced CiC effect by SAF, it is not relevant for the absolute values of our results. However, the implications of the assumption needs to be kept in mind for interpretation of the results relative to the total.

4 Results

4.1 SAF in all flights

As described in Sect. 3.2, we perform an AirClim simulation with pulse emissions in year 2030 and integrate until 2130 to obtain 100 years for climate effect analysis. The emissions include all individual flights departing from CPH as described in Sect. 3.1 on top of a global emission scenario. To put the emissions of the flights depqarting from CPH into global perspective, in our simulation they account for 0.39% of the global CO_2 and for 0.48% of the global CO2e(EAGWP100) aviation emissions. As a first step, in this section the 8 SAF scenarios (no SAF, 6%, 30%, 40%, 50%, 60%, 70% SAF blending ratios and 100% SAF) are analysed such that all the considered flights departing CPH are equipped with the respective SAF blending ratio. The flight selection for targeted SAF use and its analysis will be presented in the subsequent sections.

Fig. 5a displays the time series of the total temperature perturbation from the year 2030 emissions of all flights departing CPH without any SAF usage until year 2130. Here, all considered aviation non-CO_2 climate effects and their net effect are considered individually. A steep increase of the temperature perturbation at year 2030 can be seen here and a rapid decline of the perturbation from the non-CO_2 effects thereafter. The CH_4 and PMO effects depict a reduced warming (net-cooling), while all other effects and the net effect are clearly warming. The long lifetime of CO_2 can be observed by the very slow decrease of dT across the decades. As the temperature perturbations are much more inert than the RF perturbations (not shown), this depiction does not show that the CiC and the O_3 effects are considerably shorter than those of PMO and CH_4. For example Dahlmann et al. (2025) show this distinctively.

In Fig. 5b, the dT time series for total, CiC, and CO_2 are shown again, plus their equivalents with the difference that all flights are equipped with 6%, 30%, 40%, 50%, 60%, 70% and 100% SAF, respectively. In these scenarios, the temperature perturbations for CO_2 and CiC (and as a result from that also of the total) are reduced proportionally to the SAF blending ratio.

In a next step, the temperature perturbations (or the RF perturbation, depending on the climate metric) shown in Fig. 5 can be translated into climate effects by means of a climate metric. Climate metrics are applied to describe the effects by one number per flight scenario and climate agent and can further be used to translate the result to a CO2e. As mentioned in Sect. 3.2, we here primarily use the metric EAGWP with a 100 year time horizon, but we later on also compare the results with the climate metrics AGWP and ATR and with the time horizons 50 and 20 years. In Fig. 6 we show the CO2e that was computed using EAGWP100 for all climate agents for the 8 different SAF scenarios in our simulation.

The total CO2e of all flights departing from CPH in 2030 in our simulation is 4.86 Mt if conventional jet fuel is used, declining with increasing SAF blending ratios. As expected, a reduction happens only for CO_2 and for CiC, the CO2e of the other climate forcers remain unchanged through SAF use. Note that we neglect the effect that SAF has on the water vapour effect due to its enhanced H-content, as it is considered to be very small. According to our assumption of 20% CO_2 life-cycle

https://doi.org/10.5194/jecats-2026-15
Preprint. Discussion started: 14 August 2026

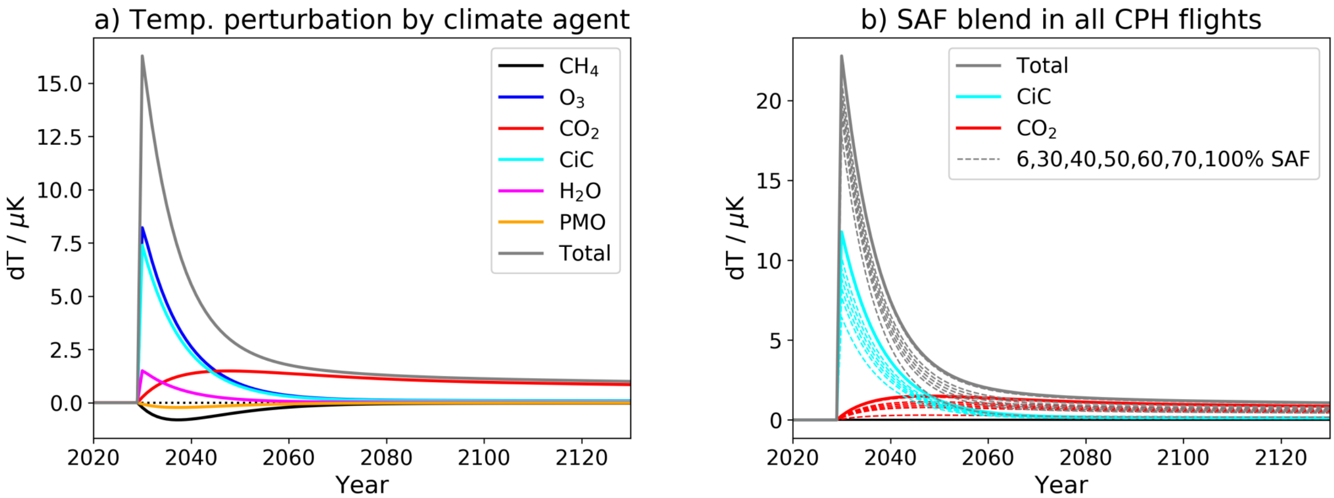

Figure 5. Temperature perturbation through pulse emission by all flights departing from CPH in 2030 simulated with AirClim until 2130 for a) all individual considered non-CO_2 effects and total as well as b) CO_2, CiC and total including 6%, 30%, 40%, 50%, 60%, 70% and 100% SAF in all flights.

emissions of SAF in comparison to Jet A-1, the CO_2 climate effect declines linearly with the SAF blending ratio down to 20% in the 100% SAF case. The CiC-based CO2e(EAGWP100) also declines fairly linearly with increasing SAF blending ratio, but with some saturation of the impact towards larger blending ratios. The reduction bases on the combination of the concavely shaped RF dependence on nvPM reduction (Eq. 2) and the convex shape of the nvPM reduction as function of the blending ratio (Fig. 4). The theoretical application of 100% SAF in all flights departing from CPH suggest a maximum reduction of the CiC climate effect by around 40% in our simulations and the total CO2e is roughly halved.

4.2 Flight selection for SAF

In the next step, we select the flights that are dedicated for SAF to climatologically achieve the largest climate benefit given the proportion of 6% SAF of the total available fuel at CPH in our 2030 scenario. For this, we follow the procedure sketched in Sect. 2, i.e. we start by assorting the flights by their CiC effect to fuel use ratio using the reference scenario with conventional jet fuel only. Then, we select the first flights in this list and replace the climate effect calculations of these particular flights with those of the scenarios with SAF. This procedure is conducted once for each of the SAF scenarios, i.e. for SAF blending ratios of 30%, 40%, 50%, 60% and 70% as well as for 100% SAF, respectively. In each case, the replacement is done until the 6% total SAF at CPH is taken up. This means that in each of the 6 cases, a different number of flights receive a SAF blend, the higher the blending ratio, the lower the number of flights. The tradeoff of number of flights with SAF blend and SAF blending ratio will be analysed. Note that due to the resulting list from the assorting method, a possible optimal SAF blending ratio in this method will to some degree depend on the particular flight plan of the airport.

https://doi.org/10.5194/jecats-2026-15
Preprint. Discussion started: 14 August 2026

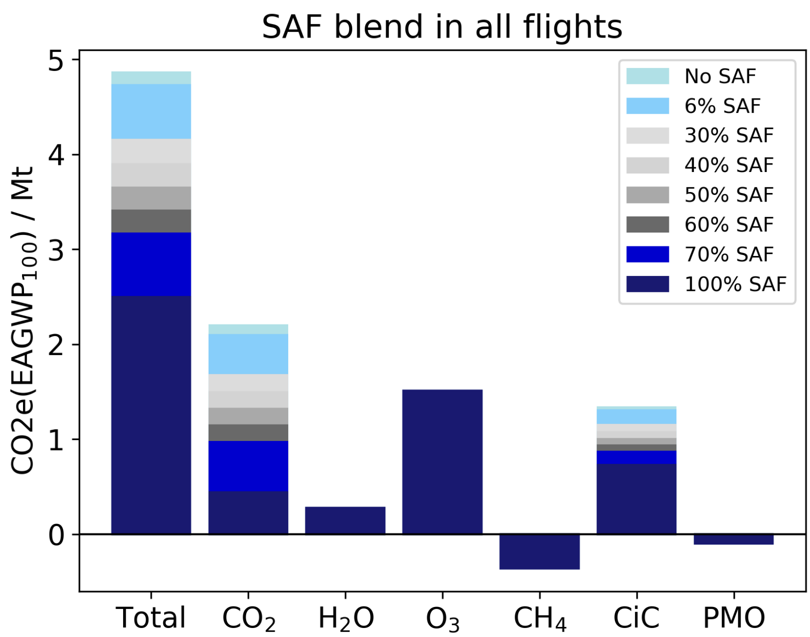

Figure 6. EAGWP100-based CO2e for all flights departing from CPH in the 2030 scenario for use of conventional jet fuel and of 6%, 30%, 40%, 50%, 60%, 70% blends as well as 100% SAF, respectively, in all flights. (Numbers are given in Tab. S1)

The CiC effect to fuel use ratio declines fairly steeply across the first few tens of flight routes for the given CPH flight plan (see Figs. S1 and S2, left panels). This means that only few flights cause the strongest CiC-induced climate effects, which corresponds to results of other studies, such as the one by Teoh et al. (2024). For overview, the numbers of flight routes, as well as actual flights and their percentage on the total for each of the SAF scenarios are provided in Tab. 1. If the last flight route in the respective list includes more than one flight, only the corresponding fraction of the flights in this flight route is considered for SAF so that the total SAF amount does not exceed the 6% of total fuel.

Table 1. Numbers of flight routes and flights that receive the respective SAF amount in the corresponding scenarios (or SAF only in the 100% scenario). Note again that in the 6% SAF case, all flights receive a 6% SAF blend.

SAF scenario	6%	30%	40%	50%	60%	70%	100%
# Flight routes	5160	570	448	416	371	304	270
% Flight routes	100	11.0	8.7	8.1	7.2	5.9	5.2
# Flights	129631	9094	7181	6691	5554	5074	4163
% Flights	100	7.0	5.5	5.2	4.3	3.9	3.2

https://doi.org/10.5194/jecats-2026-15
Preprint. Discussion started: 14 August 2026

In an effort to attribute selection of flights for targeted SAF use to more readily available quantities, we calculated the correlations of various flight variables with the EAGWP100(CiC) to fuel use ratio. Tab. 2 shows the correlation coefficients of the EAGWP100(CiC) to fuel use ratio with 7 flight variables (cruise altitude, EAGWP(CiC), mean latitude, wing span, flight distance, efficiency and fuel use) across the series of the flight routes. The corresponding time series with the assorted EAGWP100(CiC) to fuel use ratio and the variables as well as their scatter plots are provided in the Supplement (Figs. S1 and S2).

Table 2. Pearson correlation coefficients for the series of the EAGWP100(CiC) to fuel use ratio with the denoted variables across the 5160 flight routes ex CPH.

Correlation with EAGWP100(CiC)/fuel	Cruise altitude	EAGWP100 (CiC)	Mean Latitude	Wing span	Flight distance	Efficiency	Fuel use
r	0.33	0.40	0.19	-0.04	0.41	-0.23	0.23

All these variables are directly connected with the EAGWP100(CiC) to fuel use ratio, but still, all correlation coefficients are relatively low. The largest ones can be found for EAGWP100(CiC) and for flight distance with 0.40 and 0.41, respectively. Particularly for EAGWP100(CiC) this is not surprising, as it is the denominator of the ratio, but also the relation between flight distance on CiC climate impact is well-established. Despite its direct inclusion in the contrail climate effect calculation (see Sect. 3.2), the wing span does not correlate with the ratio, implying that this influence is not critical here. It is rather surprising that the general correlations are weak, also in the cases of cruise altitude, efficiency and fuel use, as all these quantities directly relate to the CiC climate effect. However, this shows that the maximum CiC climate effect per fuel is a quite complex quantity that cannot easily be determined without using a climate response model such as AirClim.

4.3 Climate benefit through targeted SAF use

For the year 2030 scenarios at CPH with targeted SAF allocation as described in Sect. 4.2, Fig. 7 displays the fleet-wide EAGWP100-based total CO2e reduction as well as separated into the CO_2 and CiC effects for the different SAF blending ratios in absolute terms. Note that for the 6% SAF blending ratio, no targeted SAF allocation but uniform distribution to all flights is performed. The larger the SAF blending ratio, the fewer flights receive SAF (see Tab. 1).

For CO_2, the fleet-wide CO2e reduction logically is the same in all SAF scenarios, here it is 106 kt CO2e, which accounts for 2.2% of the total fleet-wide CO2e. When the 6% SAF are uniformly distributed among all flights, the CiC effect reduces by about 28 kt (0.6%) leading to a total reduction of around 134 kt (2.8%) CO2e. Note again, that the CO2e of all other climate species (H_2O and NO_x effects) are not affected by SAF but do contribute to the total CO2e (4860 kt) and hence are included for the relative effect values. Targeted SAF use enhances the fleet-wide CO2e reduction through CiC to 72 kt ($\sim$1.5%) at 30% SAF blending ratio and to gradually more with increasing SAF blending ratio (and reduced number of flights with SAF) until 70% SAF blending ratio. With 100% SAF, the climate benefit is reduced again slightly, indicating that here, the benefit of the higher blending ratio does not outweigh the effect of reduced number of flights anymore. This may be related to the flatter

https://doi.org/10.5194/jecats-2026-15
Preprint. Discussion started: 14 August 2026

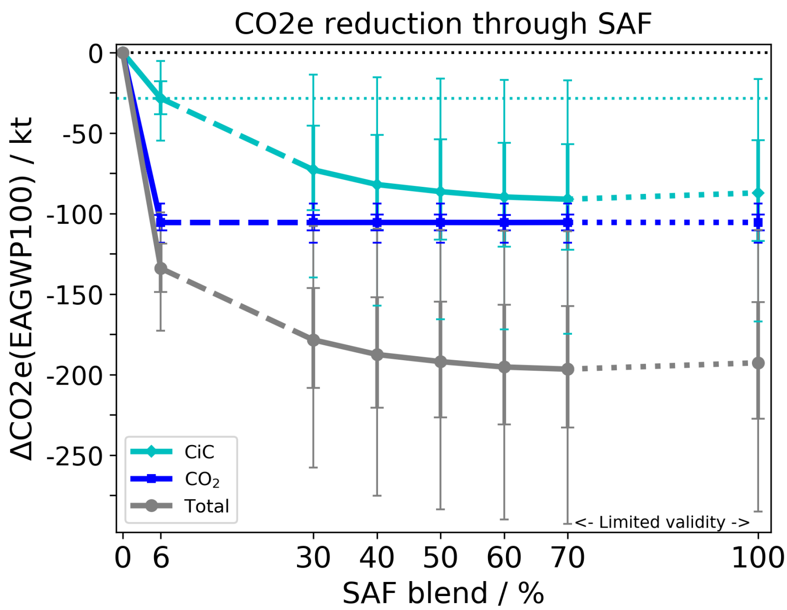

Figure 7. Fleet-wide absolute EAGWP100-based CO2e reduction for SAF use. Left part (uniform): resulting from a 6% SAF share at CPH in 2030, uniformly distributed across all flights. Right solid part: targeted SAF allocation to selected flights with blending ratios of 30%, 40%, 50%, 60% and 70% as well as with 100% SAF (dotted part of lines). The dotted cyan horizontal line marks the CiC-based CO2e reduction through 6% even distribution which denotes the reference for the other cases. The vertical lines display the uncertainty estimates as described in the text for the 50% and the 90% percentile ranges. The dashed part of the lines illustrates the break between uniform and targeted SAF use and the dotted parts the limited validity of the parameterisation above 73%. The rounded values of this plot are provided in Tabs. S2 and S3

decrease of the nvPM reduction dependence on SAF blending ratio (see Fig. 4), but as validity of the curve is limited in this region anyway, we refrain from detailed interpretation. At 70% SAF blending ratio, the fleet-wide CO2e reduction by CiC is 90 kt (1.9%), leading to a total CO2e reduction of 196 kt (4.0%). Hence, an additional 62 kt CO2e (1.3%) can potentially be saved through targeted SAF use in our 6% SAF example at CPH in 2030.

To obtain a first-order uncertainty estimate, we use uncertainty ranges of efficacy as well as influence of constituent changes on radiative forcing (see Supplement for the values) and performed a Monte-Carlo simulation with 3000 drawings for the CO2e differences of the flights. In Fig. 7, the center 50% and the 90% percentile ranges (marked by the 5%, 25%, 75% and 95% percentiles) of these distributions are shown, displaying that the uncertainties generally are large, in particular for the CiC estimations. At 50% SAF blending ratio, the 90% percentile ranges of the total CO2e difference ranges between 108 and 271 kt, so the differences between mean and the 5%/95% percentile values are slightly larger than the CO2e benefit through targeted SAF use. This also means that in the vast majority of cases (almost 90%), targeted SAF allocation does provide additional climate benefit as compared to even distribution and in some cases almost twice as much as the uncertainty. In general, it is important to include the uncertainties in cost-benefit analyses such as in (Müller et al., 2026), where the additional CO2e

https://doi.org/10.5194/jecats-2026-15
Preprint. Discussion started: 14 August 2026

benefit is monetarily juxtaposed with infrastructural and operational costs. The additional CO2e benefit through targeted SAF use at 50% SAF blending ratio is 57 kt (1.2%), and the 50% percentile range of our uncertainty estimate is ±30-35 kt, which we consider as a reasonable uncertainty range to be further used. The ΔCO2e difference between 70% and 50% SAF blending ratio is only 4.6 kt (0.1%), which, in light of the associated uncertainties, is rather small. As SAF blending is currently limited to 50% to ensure compatibility with all existing aircraft (aromatics are used to ensure seal swell), we recommend to use the 50% SAF blend results for further analyses as for example economic cost-benefit analyses (Müller et al., 2026).

Fig. 8 shows the total ΔCO2e based on EAGWP for the three time horizons 100, 50 and 20 years as well as AGWP and ATR for the recommended time horizon of 100 years.

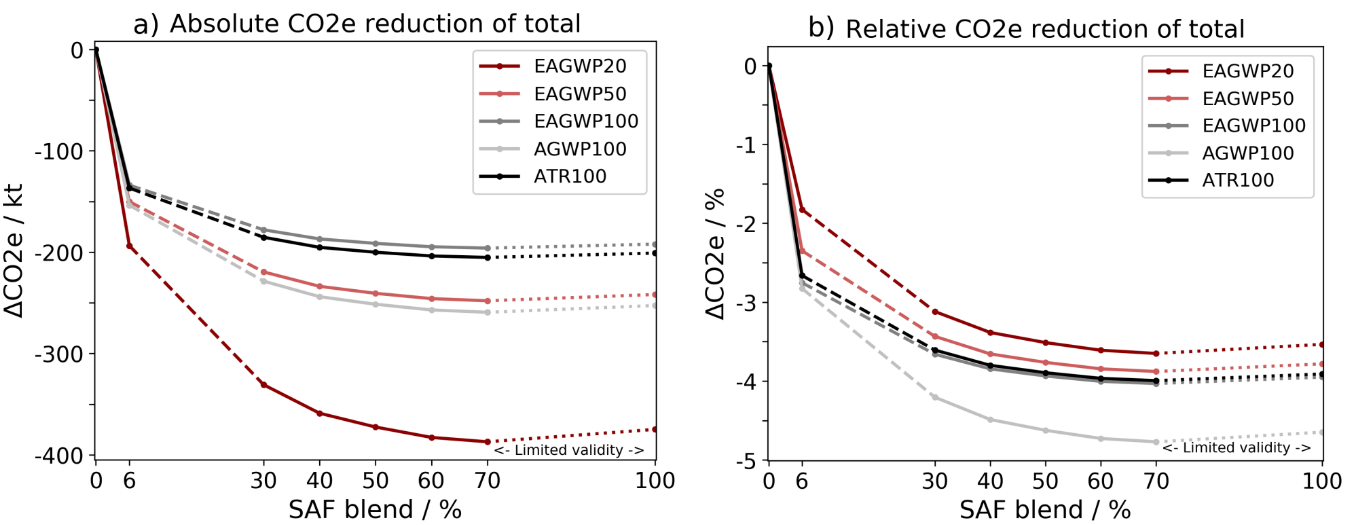

Figure 8. Absolute (a) and relative (b) fleet-wide reduction of total CO2e for different metrics and time horizons.

The choice of the time horizon is to a large extent a political choice, expressing the time a climate goal is intended to be achieved. Fig. 8a shows that the fleet-wide absolute CO2e reduction potential is largest for short time horizons (20 years) and are roughly a factor of 2 larger than the respective reductions for long time horizons (100 years). The relative changes (b) on the other hand show for the targeted SAF use between 30% and 70% roughly between 3% and 4.5% CO2e reductions with lower reductions for short time horizons. This is due to the larger absolute baseline values that emerge through lower time horizons, as the non-CO_2 effects are weighted larger here. Importantly to note is that the metrics EAGWP and ATR are basically giving the same results, whereas the impact of the integration of efficacies, hence the comparison of AGWP and EAGWP leads to larger differences. Especially the consideration of the contrail efficacy in EAGWP leads to a lower weight on contrail effects and therefore AGWP shows larger CO2e reduction potentials. As stated above, with the focus on EAGWP100 in the present study, we follow the recommendations of Megill et al. (2024) and Eichinger et al. (2025).

In this context, it is of interest to investigate the different shares of the two SAF-caused CO2e reductions (CiC and CO_2) on the total CO2e reduction for different metrics and time horizons. For this Fig. 9 shows the CiC ratio on CO2e reductions for

https://doi.org/10.5194/jecats-2026-15
Preprint. Discussion started: 14 August 2026

all SAF blending, metric and time horizon cases. Logically, here the CiC ratio always adds up to 100% together with the CO_2 ratio.

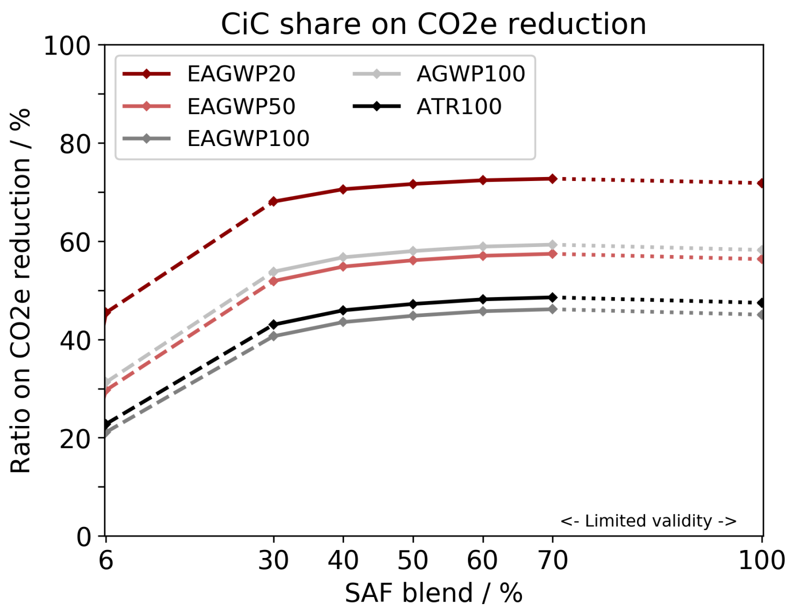

Figure 9. Ratio of CiC climate effect on absolute CO2e reduction for different SAF amounts, metrics and time horizons.

The relative importance of the CiC effect for the total CO2e reduction increases with SAF blending ratio up to the 70% blending ratio for all metrics and time horizons. As the total ΔCO_2 is constant, the relative importance basically follows the shape of the CiC curve of Fig. 7. The CiC ratio is larger for AGWP and for the shorter time horizons, for EAGWP20 it is even above 70% for the larger blending ratios. For the metrics with efficacy and larger time horizons (EAGWP100 and ATR100), the contribution of the reduction of CiC effects to the CO2e reduction reaches almost 50%, while it is only 20% for the even distribution of the 6% SAF. We can state that the share of the CiC effect of SAF on total climate benefit can be significantly enhanced by almost 30 percentage points through targeted SAF use in our example.

4.4 Reducing logistical effort

In consideration of the tradeoff between logistical effort and climate benefit from Fig. 1, we now also study the fleet-wide CO2e reduction if the flights are not sorted in the optimal way by their CiC effect to fuel use ratio, but only by their CiC effect. This means that those flights with the climatologically largest CiC climate effect are chosen for SAF uptake. Obviously, this will sacrifice some of the climate benefit, but possibly the logistical effort is reduced such to reduce operational cost at CPH.

In the 50% SAF scenario, instead of 416 different flight routes (see Tab. 1) for targeted SAF use in the CiC to fuel ratio case, only 11 different flight routes receive SAF in the assorting by largest CiC case. Fig. 10 shows that the additional CO2e benefit through CiC in the targeted SAF use cases, however, is clearly reduced. At 50% blending ratio, now only -57.4 kt ΔCO2e

https://doi.org/10.5194/jecats-2026-15
Preprint. Discussion started: 14 August 2026

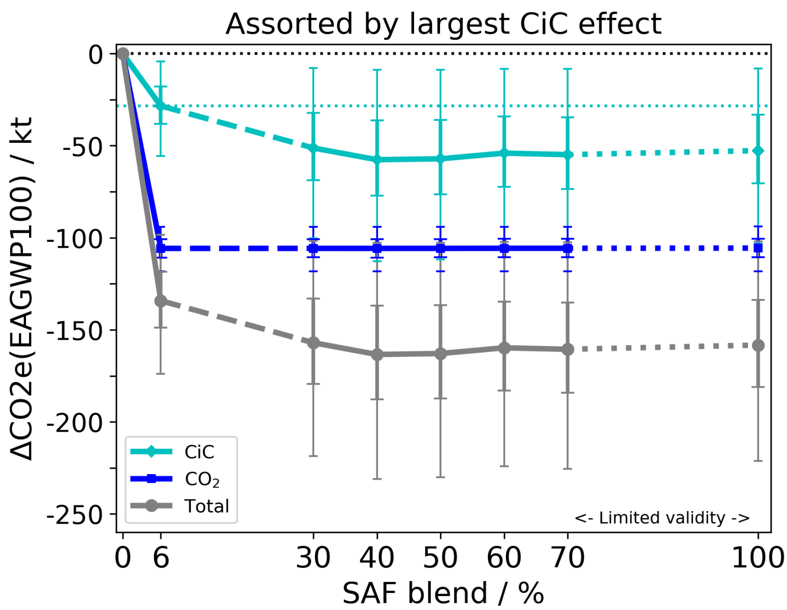

Figure 10. As Fig. 7 but for flight assorting according to EAGWP100(CiC), i.e. not divided by fuel use.

are achieved, meaning that the additional CO2e benefit is only 29.2 kt instead of 57.3 kt in the more optimal case above. Juxtaposing these numbers with the logistical cost at the airport may be one of the tasks of a dedicated cost-benefit analysis (such as Müller et al., 2026). There, an assessment of how much cost can be reduced this way could to be done, however, first attempts showed that this cost reduction is marginal. The reason is that these 11 flight routes, which are mainly long-range flights, all depart at similar time of day and hence do not reduce the number of required bowser trucks for fuelling. However, detailed analyses taking into account all influencing aspects are needed to draw clear conclusions and possibly an adaptation of the flight plan to comply with the targeted SAF use could be considered (Müller et al., 2026).

5 Discussion

Studies have shown that the lower nvPM content in SAF leads to reduced climate effect of CiC (see Burkhardt et al., 2018) and the relation between fuel characteristics, particulate emissions and the number of formed ice crystals was analysed by means of in in-flight measurements (e.g. Voigt et al., 2021). This circumstance has raised the question to what degree targeted SAF allocation to specific flights can maximise the climate benefit of SAF use (see e.g. Teoh et al., 2022b; Quante et al., 2024; Woeldgen et al., 2025). In our case study, we apply this question to the flights that depart from CPH in year 2030 when 6% SAF at European airports are made compulsory by the ReFuelEU Aviation mandate. We use the climate response model AirClim to analyse the optimal blending ratio and to quantify the potential additional climate benefit. For this, we extend the SAF parameterisation that includes a non-linear effect of nvPM on RF, by a dedicated dependence of nvPM on the SAF blending

https://doi.org/10.5194/jecats-2026-15
Preprint. Discussion started: 14 August 2026

ratio. With this tool, theoretical use of 100% SAF in all flights departing from CPH suggests a maximum reduction of the CiC climate effect by around 40% in our simulations. As we assume an 80% CO_2 life-cycle reduction of SAF, the total CO2e reduction through 100% SAF in all flights departing from CPH in our scenario is around 50%. As a matter of course, we also consider the other non-CO_2 climate effects from NO_x and from H_2O in these calculations, although there is no or only a small influence by the SAF blending.

In this work, we neglect the potential influence of volatile particulate matter (vPM) on the formation of CiC. Recent studies have shown that vPM emitted by aircraft engines such as sulphate or lubrication oil particles can act as ice nuclei causing contrail formation (Kärcher, 2018; Dischl et al., 2025; Voigt et al., 2026). This is particularly relevant for the low-soot regime, possibly leading to an underestimation of the CiC effect by lean burn engines. In the current global fleet, 10-20% of flight distance is flown by aircraft with lean burn engines and the number of aircraft equipped with lean burn engines is increasing. However, as by 2030 still the vast majority of aircraft will fly with rich burn technology and as the scientific level of understanding regarding contrail formation through vPM is still rather low, we deem our approach feasible for the time being. Still, in the coming years, this topic needs to be considered in analyses such as the present one. We also neglect the influence of SAF on the H_2O climate effect. The larger hydrogen to carbon ratio in SAF as compared to conventional jet fuel not only comes from reduced carbon content, but also from an enhanced H-content. This increases water vapour emissions and thus the direct radiative effect of water vapour. This effect however, can be considered negligible for our study, as firstly, the water vapour emission index only increases slightly through SAF and secondly, the general effect of water vapour is relatively small as compared to the others (see Fig. 6). But for specific or individual cases, this effect should be considered or at least kept in mind when interpreting climate effect results using SAF.

To select the flights eligible for targeted SAF allocation, we assort them by their CiC climate effect to fuel use ratio. This approach provides, on a climatological basis, the optimal CO2e benefit. An even advanced approach that would include weather forecasts in the SAF distribution is considered to be logistically too demanding for the time being. Other promising approaches, such as reserving SAF for night-time or winter-time (see e.g. Woeldgen et al., 2025) are not in the scope of this study and cannot be resolved in the current version of the AirClim model. Due to the high night-time CiC climate effects, this approach could additionally increase the mitigation potential of targeted SAF use and possibly even ease operational efforts. We therefore argue in support for further studies in this direction. Moreover, a multi-airport approach could interesting to investigate. As the mitigation potential of the flight schedules of one airport may be greater than that of another, transfer of larger amounts of SAF to a certain airport could prove beneficial In the optimal flight assorting of our study, the flight routes correlate with several variables such as cruise altitude, flight distance and maximum CiC climate effect. However, none of these variables correlate well and some of the suspected variables barely correlate with the CiC effect to fuel use ratio. This makes clear that for such a selection a complex climate response model has to be consulted, rather than basing it on an insufficient quantity. The assorting method itself suffers to some degree from model design details. Some flights of smaller aircraft have a large CiC effect which is not necessarily realistic. Partly this was already adjusted by use of the wing span parameterisation, but still a number of flights remain (see Fig. S2). The reason for these large CiC effects may be connected with numerical artefacts in the

https://doi.org/10.5194/jecats-2026-15
Preprint. Discussion started: 14 August 2026

ECHAM4-CCMod simulations (Burkhardt and Kärcher, 2009) the AirClim contrail response functions are based on. In future versions of AirClim, or rather OpenAirClim, this effect is expected to be improved through new GCM simulations.

As described in Sect. 3.1, the CPH emission inventory bases on the flight plan from pre-COVID year 2019, which we directly apply to year 2030. We refrained from making any future projections regarding the flight plan, as this would add a level of uncertainty that might be large enough to overshadow the effects of the targeted SAF use which is the focus of this study. Following up on the here presented results, it might be applicable to test the impact of different future flight plan scenarios on the effect of targeted SAF use and its dependencies. Possibly, flight plans can also be designed to reduce the climate impact with regard to non-CO_2 effects including SAF deployment strategies.

The result that targeted SAF use has the potential to increase the climate benefit of SAF by around 60 kt CO2e incorporates a number of further uncertainties. These include the entire calculation chain from emission uncertainties relating to the estimated amount of non-CO_2 components produced, via the meteorological uncertainties relating to specific weather situations that may not be fully covered in our climatological approach to climate response uncertainties referring to the challenges in quantifying the specific climate effects. In our first order uncertainty assessment we do not cover all of these effects, but also note that due to cross-correlations, not all should be added individually. A comprehensive depiction and inclusion of uncertainties therefore is a separate stream of work (see e.g. Lee et al., 2023). Our first order uncertainty estimate shows that the 50% percentile of the simulations is in a range where targeted SAF use leads to a considerable additional CO2e reduction. For some of the 90% percentile results, the CO2e benefit is lower than for uniform SAF distribution, but on the other end, the benefit may also be doubled. Overall, the uncertainty range can be estimated to be about as large as the additional climate benefit. Hence, in our case study a range of $\pm$30-35 kt CO2e could be recommended for further assessments of the additional CO2e benefit through targeted SAF use.

In our results, a 70% SAF blending ratio yields the largest additional CO2e benefit, although there are only small differences to the other blending ratios, especially if we consider the uncertainties. The climatically most beneficial SAF blending ratio might, however, strongly depend on the distribution of flights with regard to their CiC to fuel use ratio, or in other words to the specific flight plan of the airport. In our case at CPH, the decline of this ratio is rather steep at the beginning, meaning that few flights have a very large ratio in comparison to the majority. Other shapes of this curve might make use of smaller SAF blending ratios climatically more beneficial. Moreover, for the time being we refrain from recommending SAF blending ratios above 50% as these are not certified due to concerns of reduced seal swell.

Here, we analyse the 6% SAF scenario as mandated by ReFuelEU Aviation for 2030. Assuming the $\sim$60 kt additional climate benefit annually for the subsequent years and decades would, however, fail, as the SAF quota to be fulfilled at airports is increasing stepwise up to 70% in 2050. This means that for each of the SAF quota steps, an individual assessment needs to be carried out for integrating the effect across the coming decades. Potentially, the additional CO2e benefit from targeted SAF use will decline over the years, as a consequence of the larger general amount of SAF. Moreover, for such scenarios, not only the above mentioned flight plan developments have to be taken into account additionally, but also technological advances and shifts in fuel and SAF types. One more point to consider in a comprehensive assessment will be other mitigation strategies such as re-routing aircraft. This includes vertical or horizontal flight track adaptations to reduce the non-CO_2 effects, as for

https://doi.org/10.5194/jecats-2026-15
Preprint. Discussion started: 14 August 2026

example avoiding ice-supersaturated regions where warming contrails can form. This measure is currently widely discussed in the community (e.g. Smith et al., 2026), efforts are being taken to deploy it in trials (e.g. Sausen et al., 2024) and also the economic applicability is investigated (Niklaß et al., 2027, e.g.). Should it be feasible to do so in an extensive manner, it would counteract the additional CO2e benefit through targeted SAF use as we analysed it here. However, strategies to combine the two measures may actually lead to the biggest gain.

In addition to the physical analysis of CO2e, the economic implications of fuelling individual flights with SAF blends has to be assessed in order to practically realise targeted SAF use at CPH or any other airport. Depending on the number of flights, but also date, time of day and other variables of SAF flights and airports, a specific, possibly additional, airport wide fuelling system may have to be established. This could include pipeline systems or bowser trucks depending on pre-existing infrastructure. Investment and operating costs for such systems need to be juxtaposed with the additional CO2e benefit (Müller et al., 2026). For this, ideally the above mentioned timeframe with the stepwise increase of the SAF quota has to be considered for the additional infrastructure investment to pay dividends.

6 Conclusions

In this study, we analyse and quantify the climate-optimal way of distributing the 6% SAF as mandated by ReFuelEU Aviation for year 2030 to targeted flights departing from Copenhagen Airport (CPH). For this, we parameterise the reduction of the climate effect by contrail-induced cirrus cloudiness (CiC) through the reduced nvPM in SAF in the AirClim model and select the flights with the climatologically largest CiC effect to fuel use ratio for SAF uptake. In comparison to uniform distribution of the 6% SAF to all flights, targeted SAF use can increase the SAF climate benefit from overall ∼30 kt to ∼90 kt at CPH in year 2030, corresponding to an increase by ∼30% considering the total climate effect, including NO_x and H_2O. Therefore, the CO2e benefit from CiC through targeted SAF use is almost as large as the climate benefit of the CO_2 life-cycle reduction through SAF, which we here approximate to 80%. The impact of the CiC effect for CO2e reduction increases with SAF blending ratio up to around 70% and declines thereafter due to the tradeoff between higher SAF blending ratios and fewer flights that receive SAF. Our study bears numerous sources of uncertainties, which lead to relatively large general uncertainty of the calculated quantities. A first order uncertainty assessment shows that the uncertainties are about as large as the climate benefit from the CiC effect. This provides confidence that the measure in general leads to a positive climate impact, but it needs to be considered in quantitative cost-benefit analyses. The climatically most beneficial SAF blending ratio might strongly depend on the flight plan and the associated distribution of flights with regard to their CiC to fuel use ratio. This renders difficult transferring the results to other airports and as the CPH flight plan developments in the coming years could not be considered in this study generates additional uncertainty. Moreover, the results vary strongly for different climate metrics and time horizons. In general, the CO2e benefit is lower for climate metrics with efficacy and for longer time horizons, i.e. regarding different types of climate goals. The relative importance of the CiC effect on the total climate benefit increases with SAF blending ratio and it is larger for shorter time horizons and for metrics without efficacy. Targeted SAF use can potentially enhance the share of the CiC effect by SAF on total climate benefit by almost 30 percentage points. In our case at CPH and for the recommended 50% SAF blend

https://doi.org/10.5194/jecats-2026-15
Preprint. Discussion started: 14 August 2026

case, the relative reduction of the total CO2e ranges between -3.5% and -4.5% and 416 flight routes receive SAF. Sacrificing some of the optimal use for the sake of easier logistics by providing SAF to the flights with the largest CiC effects (without dividing by fuel) reduces the number of flight routes that receive SAF to 11, but also it halves the additional climate benefit. For a practical realisation of targeted SAF use at CPH, the economic implications of fuelling individual flights with certain SAF blends has to be assessed in a cost-benefit analysis following up on the present results. There, the specific fuelling system at the airport and numerous other factors need to be considered.

Code and data availability. Due to licensing agreements with CPH concerning the specific flight plan data and computations based thereon, the emission inventory and the AirClim results are available only upon request. The TCM, GRIDLAB and AirClim codes are proprietary.

Author contributions. RE, KD, VG, BE, WG and LM conceptualised the study. CW computed the emission inventory for the CPH network in 2019. BE designed the nvPM reduction dependence on SAF blending ratio. RE and KD performed the simulations and made the data analysis. RE wrote the paper with contributions by all authors and all authors helped with discussions.

Competing interests. Some authors are members of the editorial board of the Journal of Environmentally Compatible Air Transport System (JECATS).

Acknowledgements. We kindly thank Daniel Sauer for valuable comments on the manuscript and all data suppliers for providing the input data for aviation emission modelling (specifically ECMWF, EUROCONTROL, OpenSky Network). The CPH emission inventory has been created with elements of Base of Aircraft Data (BADA) Family 4 Release 4.2 which has been made available by EUROCONTROL to DLR (German Aerospace Center). EUROCONTROL has all relevant rights to BADA. ©2021 The European Organisation for the Safety of Air Navigation (EUROCONTROL). All rights reserved. EUROCONTROL shall not be liable for any direct, indirect, incidental or consequential damages arising out of or in connection with this product or document, including with respect to the use of BADA. Furthermore, we thank everyone involved in the ALIGHT project for support.

Financial support. This work has received funding from the European Union's Horizon 2020 research and innovation programme ALIGHT - "Copenhagen Airport: a Lighthouse for the introduction of sustainable aviation solutions for the future" under grant agreement No 957824.

https://doi.org/10.5194/jecats-2026-15
Preprint. Discussion started: 14 August 2026

References

Appleman, H.: The Formation of Exhaust Condensation Trails by Jet Aircraft, Bulletin of the American Meteorological Society, 34, 14 – 20, https://doi.org/10.1175/1520-0477-34.1.14, 1953.

Bauder, U., Hall, C., Pütz, F., Enderle, B., Le Clercq, P., and Rauch, B.: An Integrated Modelling Approach for Climate Impact Assessments in the Future Air Transportation System–Findings from the WeCare Project, in: 17th International Conference on Stability, Handling and Use of Liquid Fuels (IASH 2017), https://elib.dlr.de/193536/, 2022.

Bell, A., Mannion, L. A., Kelly, M., Ghaani, M. R., and Dooley, S.: Life cycle CO2e intensity of commercial aviation with specific sustainable aviation fuels, Applied Energy, 382, 125 075, https://doi.org/https://doi.org/10.1016/j.apenergy.2024.125075, 2025.

Bickel, M., Ponater, M., Bock, L., Burkhardt, U., and Reineke, S.: Estimating the Effective Radiative Forcing of Contrail Cirrus, Journal of Climate, 33, 1991–2005, https://doi.org/https://doi.org/10.1175/JCLI-D-19-0467.1, 2020.

Bickel, M., Ponater, M., Burkhardt, U., Righi, M., Hendricks, J., and Jöckel, P.: Contrail Cirrus Climate Impact: From Radiative Forcing to Surface Temperature Change, Journal of Climate, 38, 1895–1912, https://doi.org/https://doi.org/10.1175/JCLI-D-24-0245.1, 2025.

Bock, L. and Burkhardt, U.: Contrail cirrus radiative forcing for future air traffic, Atmos. Chem. Phys., 19, 8163–8174, https://doi.org/doi.org/10.5194/acp-19-8163-2019, 2019.

Borella, A., Steer, C., Bellouin, N., and Boucher, O.: Concept of risk-aware contrail avoidance strategies, J. Env. Com. Air Transp. Sys., 1, https://doi.org/doi.org/10.5194/jecats-1-3-2026, 2026.

Bräuer, T., Voigt, C., Sauer, D., Kaufmann, S., Hahn, V., Scheibe, M., Schlager, H., Huber, F., Le Clercq, P., Moore, R. H., and Anderson, B. E.: Reduced ice number concentrations in contrails from low-aromatic biofuel blends, Atmos. Chem. Phys., 21, 16 817–16 826, https://doi.org/10.5194/acp-21-16817-2021, 2021.

Brem, B. T., Durdina, L., Siegerist, F., Beyerle, P., Bruderer, K., Rindlisbacher, T., Rocci-Denis, S., Andac, M. G., Zelina, J., Penanhoat, O., and Wang, J.: Effects of Fuel Aromatic Content on Nonvolatile Particulate Emissions of an In-Production Aircraft Gas Turbine, Environmental Science & Technology, 49, 13 149–13 157, https://doi.org/10.1021/acs.est.5b04167, 2015.

Bruder, H., Thor, R. N., Niklaß, M., Dahlmann, K., Eichinger, R., Linke, F., Grewe, V., Matthes, S., and Unterstrasser, S.: The DLR CO_2-equivalent estimator FlightClim v1.0: an easy-to-use estimation of per flight CO_2 and non-CO_2 climate effects, Geoscientific Model Development, 19, 3551–3567, https://doi.org/10.5194/gmd-19-3551-2026, 2026.

Burkhardt, U. and Kärcher, B.: Process-based simulation of contrail cirrus in a global climate model, Journal of Geophysical Research: Atmospheres, 114, 1–13, https://doi.org/10.1029/2008JD011491, 2009.

Burkhardt, U. and Kärcher, B.: Global radiative forcing from contrail cirrus, Nature Clim. Change, 1, 54–58, https://doi.org/10.1038/nclimate1068, 2011.

Burkhardt, U., Bock, L., and Bier, A.: Mitigating the contrail cirrus climate impact by reducing aircraft soot number emissions, npj Clim Atmos Sci, 1, 37, https://doi.org/10.1038/s41612-018-0046-4, 2018.

Dahlmann, K., Grewe, V., Frömming, C., and Burkhardt, U.: Can we reliably assess climate mitigation options for air traffic scenarios despite large uncertainties in atmospheric processes?, Transportation Research Part D: Transport and Environment, 46, 40–55, https://doi.org/10.1016/j.trd.2016.03.006, 2016.

Dahlmann, K., Grewe, V., Matthes, S., and Yamashita, H.: Climate assessment of single flights: Deduction of route specific equivalent CO_2 emissions, International Journal of Sustainable Transportation, 17, 29–40, https://doi.org/10.1080/15568318.2021.1979136, 2023.

https://doi.org/10.5194/jecats-2026-15
Preprint. Discussion started: 14 August 2026

Dahlmann, K., Matthes, S., and Grewe, V.: Conversion of climate metrics for policy applications, Preprint, Submitted to Meteorologische Zeitschrift, pp. 1–34, https://doi.org/10.5281/zenodo.16355780, 2025.

Deidewig, F., Doepelheuer, A., and Lecht, M.: Methods to Assess Aircraft Engine Emissions in Flight, in: 20th Congress of the Int. Council of the Aeronautical Sciences 1996 (ICAS), Sorrento, Italy, 1996.

Dischl, R., Märkl, R., Sauer, D., Voigt, C., Harlaß, T., Scheibe, M., Hahn, V., Kaufmann, S., Marsing, A., Dörnbrack, A., Roiger, A., Yu, F., Gauthier, M., Renard, C., Swann, P., Johnson, M., Ahrens, D., Sallinen, R., Eckel, G., and Le Clercq, P.: Fuel sulfur content can modulate contrail ice crystal numbers, Commun Earth Environ, 6, 902, https://doi.org/10.1038/s43247-025-02951-5, 2025.

EASA: Introduction to the ICAO Engine Emissions Databank, Tech. Rep. TE.GEN.00301-006, European Union Aviation Safety Agency (EASA), Cologne, Germany, https://www.easa.europa.eu/en/downloads/45576/en, accessed: 2026-04-28, 2023.

Eichinger, R., Dahlmann, K., Grewe, V., Matthes, S., Niklaß, M., Lau, A., Zengerling, Z., Dietmüller, S., Völk, S., Megill, L., Voigt, C., Piontek, D., Kirschler, S., Plohr, M., Beckmann, B.-R., Schlemmer, L., Hanst, M., Köhler, C., Hollborn, S., Seifert, A., and Fundel, F.: Reference set of technical specifications for the MRV, Tech. Rep. EC-CLIMA/2024/NP/0014, Deutsches Zentrum für Luft- und Raumfahrt e.V., Linder Höhe, Cologne, https://climate.ec.europa.eu/document/download/735ae93d-d49d-46e0-b95b-48c36230ad57_en?filename=policy_ets_aviation_reference_set_technical_specifications_non_co2_mrv_en.pdf, 2025.

Enderle, B., Rauch, B., Hall, C., and Bauder, U.: A proposed Digital Twin concept for the smart utilization of Sustainable Aviation Fuels, AIAA SciTech, Forum, https://doi.org/10.2514/6.2022-1294, 2022.

European-Commission: Commission Implementing Regulation (EU) 2023/2405, https://eur-lex.europa.eu/legal-content/EN/TXT/?uri=CELEX%3A32023R2405, a REGULATION (EU) 2023/2405 of the European Parliament and of the Council of 18 October 2023 on ensuring a level playing field for sustainable air transport (ReFuelEU Aviation), 2023.

European-Commission: Commission Implementing Regulation (EU) 2024/2493, https://eur-lex.europa.eu/eli/reg_impl/2024/2493/oj, amending Implementing Regulation (EU) 2018/2066 as regards updating the monitoring and reporting of greenhouse gas emissions pursuant to Directive 2003/87/EC of the European Parliament and of the Council, 2024.

Gierens, K., Sausen, R., Bauder, U., Eckel, G., Großmann, K., Le Clercq, P., Lee, D., Rauch, B., Sauer, D., Voigt, C., and Schmidt, A.: Influence of aviation fuel composition on the formation and lifetime of contrails: a literature review, Concawe Report, https://doi.org/ISBN: 978-2-87567-181-3, 2024.

Grewe, V. and Stenke, A.: AirClim: an efficient tool for climate evaluation of aircraft technology, Atmospheric Chemistry and Physics, 8, 4621–4639, https://doi.org/10.5194/acp-8-4621-2008, 2008.

Grewe, V., Gangoli Rao, A., Grönstedt, T., Xisto, C., Linke, F., Melkert, J., Middel, J., Ohlenforst, B., Blakey, S., Christie, S., Matthes, S., and Dahlmann, K.: Evaluating the climate impact of aviation emission scenarios towards the Paris agreement including COVID-19 effects, Nature Communications, 12, 3841, https://doi.org/10.1038/s41467-021-24091-y, 2021.

Hersbach, H., Bell, B., Berrisford, P., Biavati, G., Horányi, A., Muñoz Sabater, J., Nicolas, J., Peubey, C., Radu, R., Rozum, I., Schepers, D., Simmons, A., Soci, C., Dee, D., and Thépaut, J.-N.: ERA5 hourly data on pressure levels from 1940 to present. Copernicus Climate Change Service (C3S) Climate Data Store (CDS), https://doi.org/10.24381/cds.bd0915c6, accessed on 15-11-2024, 2023.

Hofer, S., Gierens, K., and Rohs, S.: Contrail formation and persistence conditions for alternative fuels, Meteorologische Zeitschrift, 33, 43–49, https://doi.org/10.1127/metz/2024/1178, 2024.

IATA: Sustainable Aviation Fuels Fact Sheet 5, https://www.iata.org/contentassets/d13875e9ed784f75bac90f000760e998/saf-and-sustainability.pdf, accessed: 2025-10-09, 2018.

https://doi.org/10.5194/jecats-2026-15
Preprint. Discussion started: 14 August 2026

ICAO: Manual of the ICAO Standard Atmosphere: Extended to 80 Kilometres (262 500 Feet), Doc (International Civil Aviation Organization), International Civil Aviation Organization, https://books.google.de/books?id=4RgKxAEACAAJ, 1993.

ICAO: Annex 16 to the Convention on International Civil Aviation – Environmental Protection – Volume II: Aircraft Engine Emissions. 3. Edition, Tech. rep., International Civil Aviation Organization, 2008.

ICAO: ICAO Engine Exhaust Emissions Data; Databank, Doc 9646-AN/943, Issue 18; ICAO: Montreal, QC, Canada, 2012, https://www.easa.europa.eu/domains/environment/icao-aircraft-engine-emissions-databank, accessed: 2024-06-19, 2012.

Kärcher, B.: Formation and radiative forcing of contrail cirrus, Nature Communications, 9, 1824, https://doi.org/10.1038/s41467-018-04068-0, 2018.

Lee, D., Fahey, D., Skowron, A., Allen, M., Burkhardt, U., Chen, Q., Doherty, S., Freeman, S., Forster, P., Fuglestvedt, J., Gettelman, A., De León, R., Lim, L., Lund, M., Millar, R., Owen, B., Penner, J., Pitari, G., Prather, M., Sausen, R., and Wilcox, L.: The contribution of global aviation to anthropogenic climate forcing for 2000 to 2018, Atmospheric Environment, 244, 117 834, https://doi.org/10.1016/j.atmosenv.2020.117834, 2021.

Lee, D. S., Allen, M. R., Cumpsty, N., Owen, B., Shine, K. P., and Skowron, A.: Uncertainties in mitigating aviation non-CO2 emissions for climate and air quality using hydrocarbon fuels, Environ. Sci.: Atmos., 3, 1693–1740, https://doi.org/10.1039/D3EA00091E, 2023.

Linke, F.: Environmental Analysis of Operational Air Transportation Concepts, Ph.D. thesis, Hamburg University of Technology, 2016.

Linke, F., Grewe, V., and Gollnick, V.: The Implications of Intermediate Stop Operations on Aviation Emissions and Climate, Meteorologische Zeitschrift, 26, 697–709, https://doi.org/10.1127/metz/2017/0763, 2017.

Märkl, R. S., Voigt, C., Sauer, D., Dischl, R. K., Kaufmann, S., Harlaß, T., Hahn, V., Roiger, A., Weiß-Rehm, C., Burkhardt, U., Schumann, U., Marsing, A., Scheibe, M., Dörnbrack, A., Renard, C., Gauthier, M., Swann, P., Madden, P., Luff, D., Sallinen, R., Schripp, T., and Le Clercq, P.: Powering aircraft with 100 % sustainable aviation fuel reduces ice crystals in contrails, Atmospheric Chemistry and Physics, 24, 3813–3837, https://doi.org/10.5194/acp-24-3813-2024, 2024.

Matthes, S., Lim, L., Burkhardt, U., Dahlmann, K., Dietmüller, S., Grewe, V., Haslerud, A. S., Hendricks, J., Owen, B., Pitari, G., Righi, M., and Skowron, A.: Mitigation of non-CO_2 aviation's climate impact by changing cruise altitudes, Aerospace, 8, 36, https://doi.org/10.3390/aerospace8020036, 2021.

Megill and Grewe, V.: Investigating the limiting aircraft-design-dependent and environmental factors of persistent contrail formation, Atmos. Chem. Phys., 25, 4131–4149, https://doi.org/10.5194/acp-25-4131-2025, 2025.

Megill, L., Deck, K., and Grewe, V.: Alternative climate metrics to the Global Warming Potential are more suitable for assessing aviation non-CO2 effects, Commun Earth Environ, 5, 249, https://doi.org/10.1038/s43247-024-01423-6, 2024.

Moore, R., Thornhill, K., Weinzierl, B., Sauer, D., D'Ascoli, E., Kim, J., Lichtenstern, M., Scheibe, M., Beaton, B., Beyersdorf, A., Barrick, J., Bulzan, D., Corr, C., Crosbie, E., Jurkat, T., Martin, R., Riddick, D., Shook, M., Slover, G., Voigt, C., White, R., Winstead, E., Yasky, R., Ziemba, L., Brown, A., H., S., and Anderson, B.: Biofuel blending reduces particle emissions from aircraft engines at cruise conditions, Nature, 543, 411–415, https://doi.org/10.1038/nature21420, 2017.

Müller, L., Kumar, S., Grimme, W., Maertens, S., Eichinger, R., Enderle, B., Weder, C., Dahlmann, K., and Grewe, V.: Targeted Use of Sustainable Aviation Fuel at Airports for Climate Mitigation: A Cost-Benefit Perspective, submitted, 2026.

Niklaß, M., Zengerling, Z., Mendiguchía Meuser, M., Eichinger, R., Ehlers, T., Lau, A., Yin, F. Stefanidi, A., and Grewe, V.: Impact of Non-CO_2 Pricing on Routing and Ticket Fares in Aviation: Strategies to Address Uncertainties in Climate Policies, Submitted to Meteorologische Zeitschrift, preprint, https://doi.org/10.5281/zenodo.15438171, 2027.

Nuic, A., Poles, D., and Mouillet, V.: BADA: An advanced aircraft performance model for present and future ATM systems, International Journal of Adaptive Control and Signal Processing, 24, 850–866, https://doi.org/10.1002/acs.1176, 2010.

openflights.org: Airport database, https://openflights.org/data.php#airport, accessed: 2026-04-28, 2026.

Ponater, M., Pechtl, S., Sausen, R., Schumann, U., and Hüttig, G.: Potential of the cryoplane technology to reduce aircraft climate impact: A state-of-the-art assessment, Atmospheric Environment, 40, 6928–6944, https://doi.org/https://doi.org/10.1016/j.atmosenv.2006.06.036, 2006.

Quante, G., Voigt, C., and Kaltschmitt, M.: Targeted use of paraffinic kerosene: Potentials and implications, Atmospheric Environment: X, 23, 100 279, https://doi.org/https://doi.org/10.1016/j.aeaoa.2024.100279, 2024.

Quante, G., Enderle, B., Laybourn, P., Holm, P. W., Andersen, L. W., Voigt, C., and Kaltschmitt, M.: Segregated supply of Sustainable Aviation Fuel to reduce contrail energy forcing – demonstration and potentials, Journal of the Air Transport Research Society, 4, 100 049, https://doi.org/https://doi.org/10.1016/j.jatrs.2024.100049, 2025.

Rap, A., Forster, P. M., Haywood, J. M., Jones, A., and Boucher, O.: Estimating the climate impact of linear contrails using the UK Met Office climate model, Geophysical Research Letters, 37, https://doi.org/https://doi.org/10.1029/2010GL045161, 2010.

Riahi, K., van Vuuren, D. P., Kriegler, E., Edmonds, J., O'Neill, B. C., Fujimori, S., Bauer, N., Calvin, K., Dellink, R., Fricko, O., Lutz, W., Popp, A., Crespo Cuaresma, J., KC, S., Leimbach, M., Jiang, L., Kram, T., Rao, S., Emmerling, J., Ebi, K., Hasegawa, T., Havlik, P., Humpenöder, F., Da Silva, L. A., Smith, S., Stehfest, E., Bosetti, V., Eom, J., Gernaat, D., Masui, T., Rogelj, J., Strefler, J., Drouet, L., Krey, V., Luderer, G., Harmsen, M., Takahashi, K., Baumstark, L., Doelman, J. C., Kainuma, M., Klimont, Z., Marangoni, G., Lotze-Campen, H., Obersteiner, M., Tabeau, A., and Tavoni, M.: The Shared Socioeconomic Pathways and their energy, land use, and greenhouse gas emissions implications: An overview, Global Environmental Change, 42, 153–168, https://doi.org/https://doi.org/10.1016/j.gloenvcha.2016.05.009, 2017.

Richardson, T. B., Forster, P. M., Smith, C. J., Maycock, A. C., Wood, T., Andrews, T., Boucher, O., Faluvegi, G., Fläschner, D., Hodnebrog, O., Kasoar, M., Kirkevåg, A., Lamarque, J.-F., Mülmenstädt, J., Myhre, G., Olivié, D., Portmann, R. W., Samset, B. H., Shawki, D., Shindell, D., Stier, P., Takemura, T., Voulgarakis, A., and Watson-Parris, D.: Efficacy of Climate Forcings in PDRMIP Models, Journal of Geophysical Research: Atmospheres, 124, 12 824–12 844, https://doi.org/https://doi.org/10.1029/2019JD030581, 2019.

Righi, M., Ehrenberger, S., Brinkop, S., Hendricks, J., Hellekes, J., Banyś, P., Dasgupta, I., Draheim, P., Fitz, A., Löber, M., Pregger, T., Scholz, Y., Schulz, A., Suhr, B., Thomsen, N., Weder, C. M., Berster, P., Clococeanu, M., Gelhausen, M., Lau, A., Linke, F., Matthes, S., and Zengerling, Z. L.: The ELK global emission inventory for the transport sectors, Earth System Science Data, 18, 1619–1664, https://doi.org/10.5194/essd-18-1619-2026, 2026.

Sabre MI: Data Based on Market Information Data Tapes (MIDT), https://www.sabre.com/products/suites/pricing-and-revenue-optimization/market-intelligence/, accessed: 2024-11-30, 2019.

Sausen, R., Hofer, S., Gierens, K., Bugliaro, L., Ehrmanntraut, R., Sitova, I., Walczak, K., Burridge-Diesing, A., Bowman, M., and Miller, N.: Can we successfully avoid persistent contrails by small altitude adjustments of flights in the real world?, Meteorologische Zeitschrift, 33, 83–98, https://doi.org/10.1127/metz/2023/1157, 2024.

Schaefer, M. and Bartosch, S.: Overview on fuel flow correlation methods for the calculation of NOx, CO and HC emissions and their implementation into aircraft performance software, Tech. Rep. IB-325-11-13, German Aerospace Center (DLR), Cologne, Germany, 2013.

https://doi.org/10.5194/jecats-2026-15
Preprint. Discussion started: 14 August 2026

Schäfer, M., Strohmeier, M., Lenders, V., Martinovic, I., and Wilhelm, M.: Bringing up OpenSky: a large-scale ADS-B sensor network for research, in: Proceedings of the 13th International Symposium on Information Processing in Sensor Networks, IPSN '14, p. 83–94, IEEE Press, ISBN 9781479931460, 2014.

Schmidt, E.: Die Entstehung von Eisnebel aus den Auspuffgasen von Flugmotoren, Schriften der Deutschen Akademie der Luftfahrtforschung, 5, 1–15, 1941.

Smith, J., Grobler, C., Hodgson, P., Mukhopadhaya, J., Shapiro, M. L., Mirolo, M., Stettler, M. E. J., D., E. S., and Barrett, S. R. H.: The climate opportunities and risks of contrail avoidance, Nat Commun, 17, https://doi.org/10.1038/s41467-026-68784-8, 2026.

Staniaszek, Z., Hauglustaine, D. A., Cohen, Y., Skowron, A., Matthes, S., Thor, R., and Lund, M. T.: Impact of future aircraft NOx emissions on atmospheric composition and climate: dependence on background conditions, Atmos. Chem. Phys., 26, 7985–7999, https://doi.org/10.5194/acp-26-7985-2026, 2026.

Stenke, A., Grewe, V., and Ponater, M.: Lagrangian transport of water vapor and cloud water in the ECHAM4 GCM and its impact on the cold bias, Climate Dynamics, 31, 491–506, https://doi.org/10.1007/s00382-007-0347-5, 2008.

Strohmeier, M., Olive, X., Lübbe, J., Schäfer, M., and Lenders, V.: Crowdsourced air traffic data from the OpenSky Network 2019–2020, Earth Syst. Sci. Data, 13, 357–366, https://doi.org/10.5194/essd-13-357-2021, 2021.

Swaid, M., Linke, F., and Gollnick, V.: A Methodology for Efficient Statistical Analysis of Air Distance in Aviation, in: AIAA AVIATION FORUM AND ASCEND 2024, https://doi.org/10.2514/6.2024-3850, 2024.

Teoh, R., Schumann, U., Gryspeerdt, E., Shapiro, M., Molloy, J., Koudis, G., Voigt, C., and Stettler, M. E. J.: Aviation contrail climate effects in the North Atlantic from 2016 to 2021, Atmospheric Chemistry and Physics, 22, 10 919–10 935, https://doi.org/10.5194/acp-22-10919-2022, 2022a.

Teoh, R., Schumann, U., Voigt, C., Schripp, T., Shapiro, M., Engberg, Z., Molloy, J., Koudis, G., and Stettler, M. E. J.: Targeted Use of Sustainable Aviation Fuel to Maximize Climate Benefits, Environmental science and technology, 56, 17 246–17 255, https://doi.org/10.1021/acs.est.2c05781, 2022b.

Teoh, R., Engberg, Z., Schumann, U., Voigt, C., Shapiro, M., Rohs, S., and Stettler, M. E. J.: Global aviation contrail climate effects from 2019 to 2021, Atmospheric Chemistry and Physics, 24, 6071–6093, https://doi.org/10.5194/acp-24-6071-2024, 2024.

Unterstrasser, S. and Görsch, N.: Aircraft-type dependency of contrail evolution, Journal of Geophysical Research: Atmospheres, 119, 14,015–14,027, https://doi.org/https://doi.org/10.1002/2014JD022642, 2014.

Urjais, D.: DDR2 Reference Manual for Airline Users (ed. 2.9.11), Tech. rep., EUROCONTROL, Brussels, Belgium, https://www.eurocontrol.int/ddr, 2022.

Voigt, C., Kleine, J., Sauer, D., Moore, R. H., Bräuer, T., Clercq, P. L., Kaufmann, S., Scheibe, M., Jurkat-Witschas, T., Aigner, M., Bauder, U., Boose, Y., Borrmann, S., Crosbie, E., Diskin, G. S., DiGangi, J., Hahn, V., Heckl, C., Huber, F., Nowak, J. B., Rapp, M., Rauch, B., Robinson, C., Schripp, T., Shook, M., Winstead, E., Ziemba, L., Schlager, H., and Anderson, B. E.: Cleaner burning aviation fuels can reduce contrail cloudiness, Commun Earth Environ, 2, https://doi.org/10.1038/s43247-021-00174-y, 2021.

Voigt, C., Märkl, R., Sauer, D., Dischl, R., Renard, C., Seeliger, K., Yu, F., Kaufmann, S., Bräuer, T., Jurkat-Witschas, T., Le Chenadec, G., Moreau, J., Requena-Esteban, E., Bonne, N., Vals, M., Roche, A., Zelina, J., Dörnbrack, A., Eirenschmalz, L., Heckl, C., Horst, E., Lichtenstern, M., Marsing, A., Neumann, G., Roiger, A., Scheibe, M., Stock, P., Giez, A., Eckel, G., and Le Clercq, P.: Substantial aircraft contrail formation at low soot emission levels, Nature, 652, 112–118, https://doi.org/doi.org/10.1038/s41586-026-10286-0, 2026.

von Bonhorst, G., Maizet, M., and Gierens, K.: On contrail prediction under realistic weather forecast uncertainty using the example of WAWFOR data, Meteorologische Zeitschrift, Early Access Article, 1–15, https://doi.org/10.1127/metz/1251, 2025.

https://doi.org/10.5194/jecats-2026-15
Preprint. Discussion started: 14 August 2026

Wilkerson, J. T., Jacobson, M. Z., Malwitz, A., Balasubramanian, S., Wayson, R., Fleming, G., Naiman, A. D., and Lele, S. K.: Analysis of emission data from global commercial aviation: 2004 and 2006, Atmospheric Chemistry and Physics, 10, 6391–6408, https://doi.org/10.5194/acp-10-6391-2010, 2010.

Woeldgen, E., Teoh, R., Stettler, M. E. J., and Malina, R.: Sustainable Aviation Fuel Deployment Strategies in Europe: Supply Chain Implications and Climate Benefits, Environmental science and technology, 59, 12 447–12 457, https://doi.org/10.1021/acs.est.5c02364, 2025.

Zengerling, Z. L., Linke, F., Weder, C. M., and Dahlmann, K.: Climate-Optimised Intermediate Stop Operations: Mitigation Potential and Differences from Fuel-Optimised Configuration, Appl. Sci., 12, https://doi.org/10.3390/app122312499, 2022.